2.3.2 O/H Isotope Composition of Hot Spring Water

The D/H and $^{18}O/^{16}O$ values of the hot spring water in the survey area range from −70.8 to −55.2°/$_{oo}$ and from −10.9 to −7.6°/$_{oo}$, respectively. Figs. III−2−18 and III−2−19 show the relative position of these waters as plotted on the figure of Hoefs (1980). Based on the isotopic values of the samples, the origin of the hot spring water may be attributed to meteoric water. This observation is more apparent from the values of $\delta\ ^{18}O$.

Fig. III−2−20 shows the relation of isotopic composition between oxygen and hydrogen. The meteoric water lines in the Figure are:

$D = 8.\delta^{18}O + 10$	Precipitation on the Pacific Ocean (Craig, 1961).
$D = 8.\delta^{18}O + 26$	Precipitation on the Japan Sea (Sakai/Ohki, 1978)

In the Figures, the values of O/H isotopes of the hot spring water samples collected at 3,150 level (Nos. 9, 10 and 11), 2,900 level (Nos. 7 and 8), 2,300 No. 14), in crosscuts (No. 15) of Acupan mine and along the Ambalanga river banks fall in a straight line, which runs parallel to the model line formulated by Craig (1961) though with a slight shift to the left of the model line. It is assumed that the samples collected could have originated from meteoric sources. On the other hand, the values of D/H and $^{18}O/^{16}O$ of the samples (last year, 1983) taken from a creek located east of Dulapirip (DA-ST) and based on the precipitation (PRE) data collected at the eastern part of Baguio City, indicate −71.0°/$_{oo}$, −10°/$_{oo}$ (DA-ST) and −66.9°/$_{oo}$ (PRE), respectively. These values roughly fall on the Craig's line. When comparing these situations, the analyzed values of the samples more or less have shifted to the left presumably due to some seasonal varations in the degree of precipitation. The hot spring water samples collected at 3,300 level (Nos. 12, 13 and BA-1), 3,150 level (BA-2) and 2,900 level (No. 6) have indicated some oxygen shifts which point to possible chemical interactions between upflowing thermal water solution and the country rock. It is believed that the hot spring water found in Acupan is mainly heated surface water being contaminated by the reservoir fluid.

$\delta^{18}O$ and δD for Nos. 3, 4 and 5 of 2,900 level show different compositions as compared with the other samples. However, the isotope compositions of these water samples are relatively similar with those of the precipitation in Japan Sea coast (Sakai/ohki, 1978). The dispersion of $\delta^{18}O$ values among the nearby samples is also worthy to note. For example, samples Nos. 9, 10 and 11 (all taken at level −3,150 which were collected at various distance of 300–400 meters away) fall on the local meteoric water line. It is presumed that the fluid is mainly meteoric water which flows along fractures of the mineralized zone and subsequently undergo partial isotopic fractionation.

Fig. III–2–21 shows the distribution of the $\delta^{18}O$ values of hot spring water. Assuming that the $\delta^{18}O$ value increases under the condition of higher temperature and longer time for chemical interaction between the thermal fluid and reservoir rock, it is probable that the distribution of high $\delta^{18}O$ values is related to the dilution of thermal fluid coming from depth as shown in Fig. III–2-21. High concentration of $\delta^{18}O$ values in the Balatoc plug of Acupan mine and in the Itogon plug generally persist northeasterly. In the case of sample No. 6 taken at 2,900 level there is an oxygen shift which represents the upper limit of thermal fluid distribution in the area.

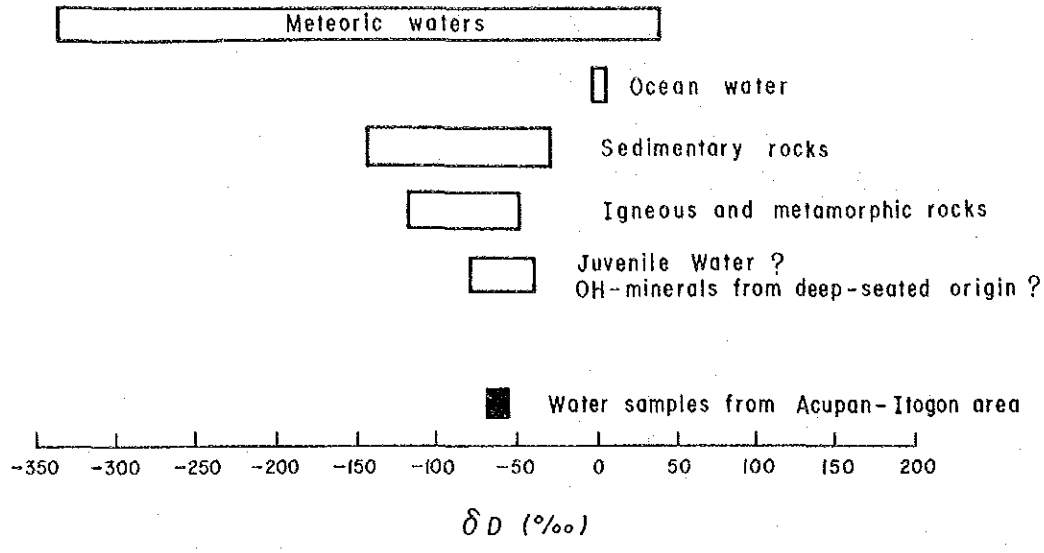

Fig. Ⅲ-2-18 D/H Ratios of some Geologically Important Materials, Quoted from Hoefs (1980)

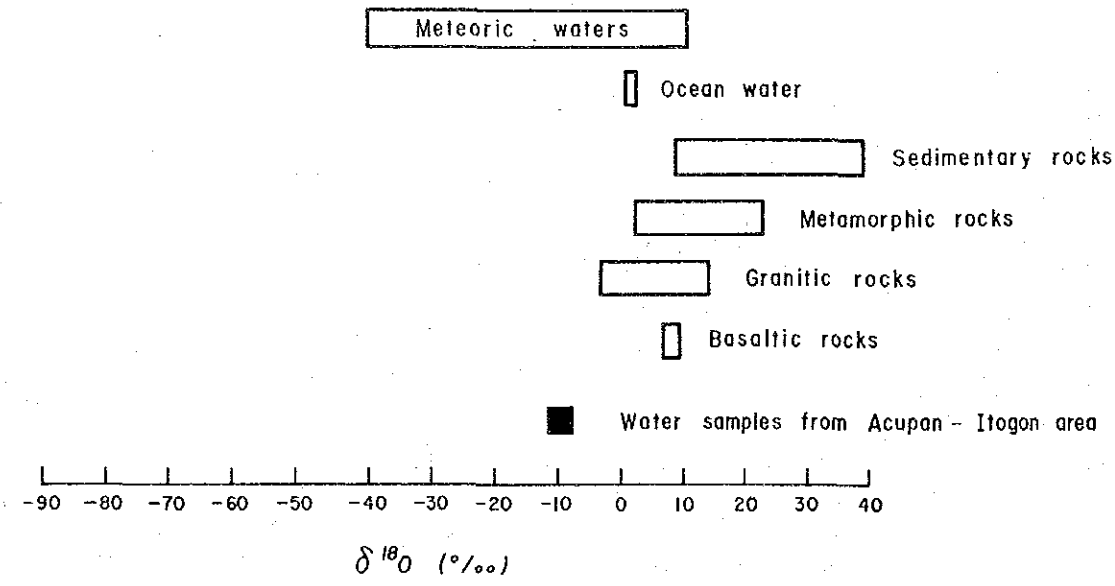

Fig. Ⅲ-2-19 $^{18}O/^{16}O$ Ratios of some Important Oxygen-containing Compounds, Quoted from Hoefs (1980)

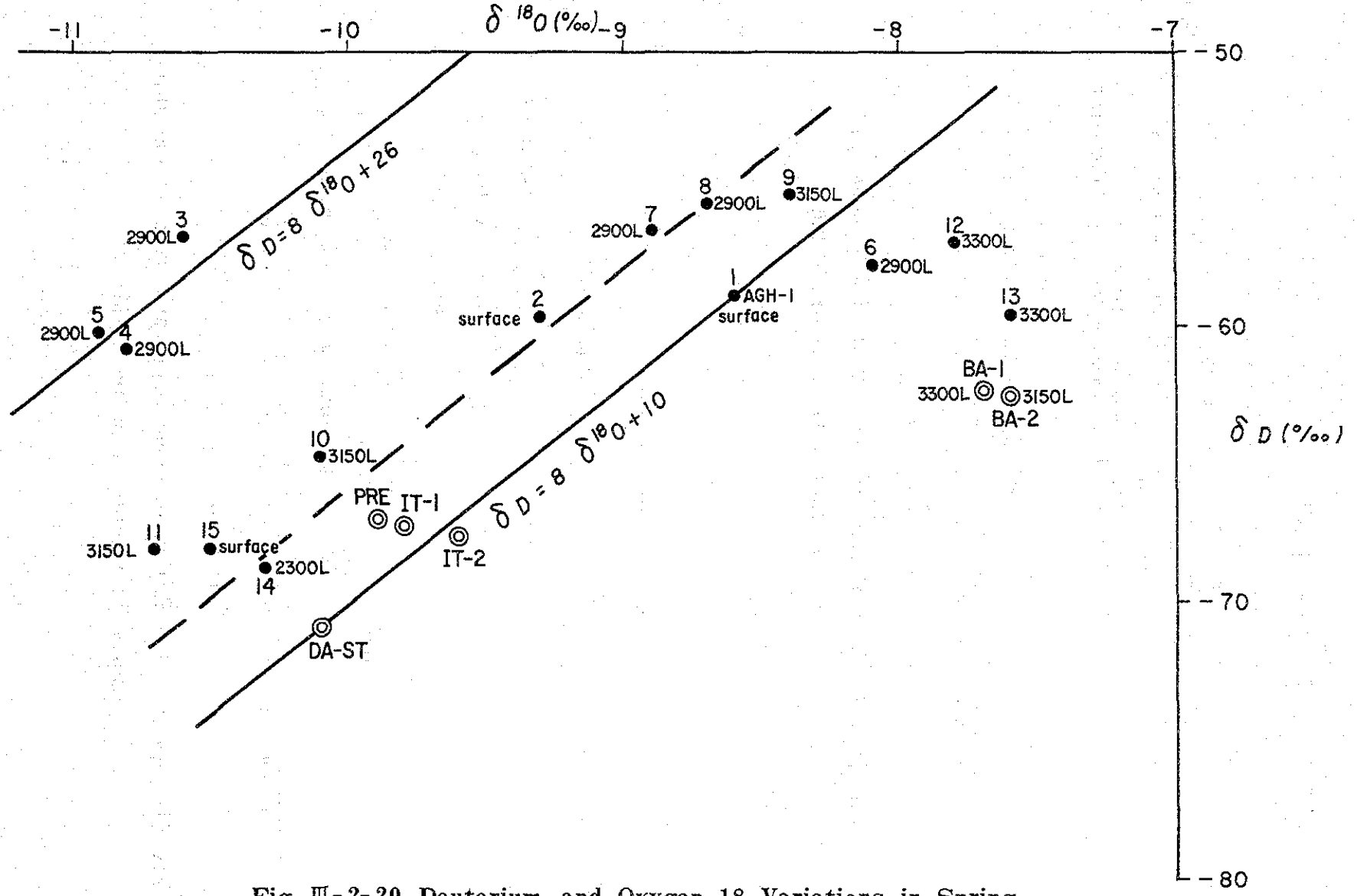

Fig. Ⅲ-2-20 Deuterium and Oxygen-18 Variations in Spring Water Samples

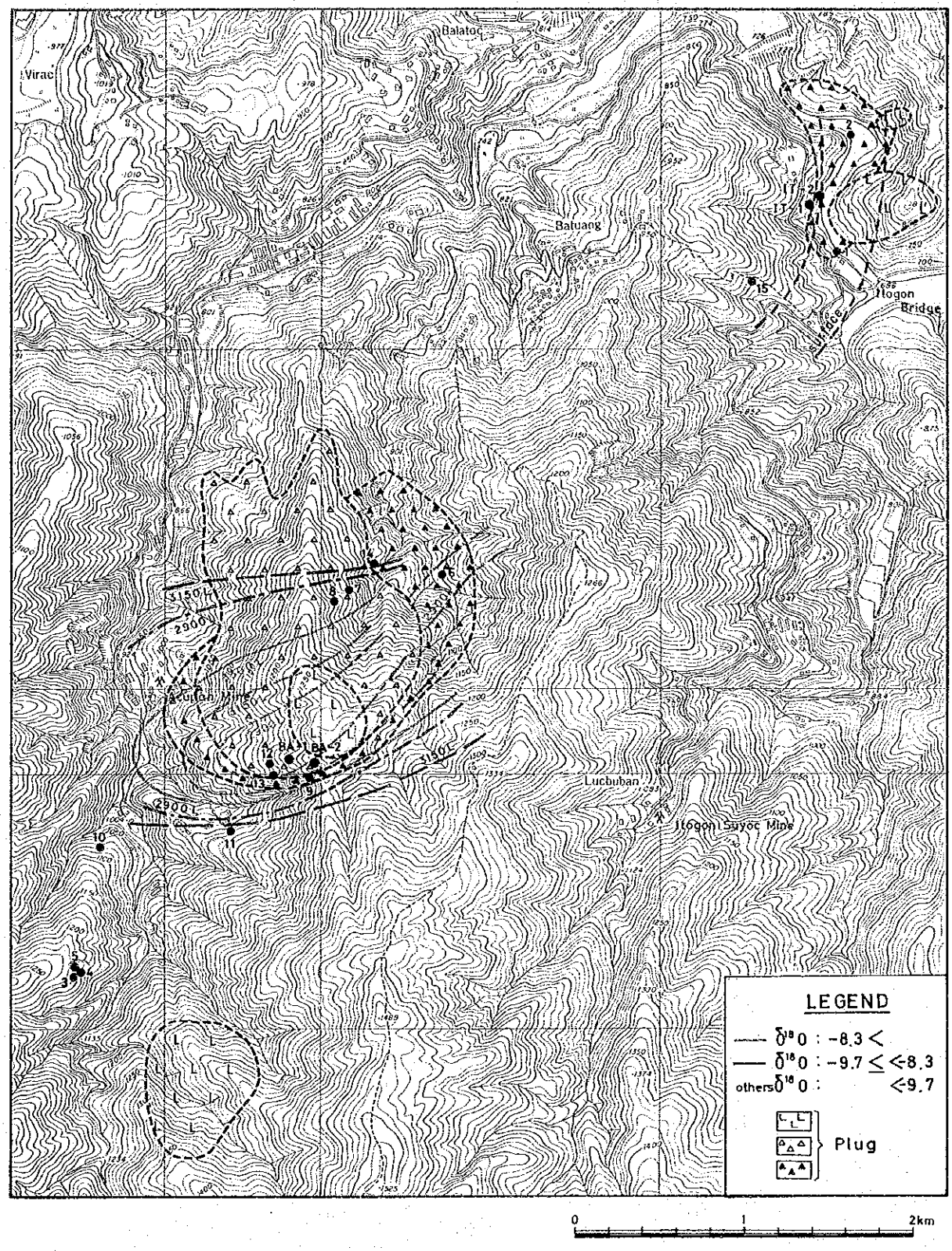

Fig. Ⅲ-2-21 Contour Map of $\delta^{18}O$ Values of Spring Water Samples

2.4 Evaluation of Results of Geochemical Exploration

The results of the Phase-I and -II survey activity carried out in the Acupan-Itogon geothermal prospect yeild the following findings:

The ground geochemical survey (involving measurements of soil temperatures, mercury concentration in soil and Radon gas concentration in soil-air) indicates significant geochemical anomalous zone trending northeasterly and covers the area bounded by the Acupan mine and Itogon plug.

The temperature of the spring waters (of neutral pH) discharging in Acupan underground mine and near the Itogon bridge is higher in nearer to the dacite plugs. The underground temperatures estimated from SiO_2 and Na-K-Ca geothermometers range from 147–229°C and 193–236°C, respectively. Based on chemistry, the spring waters may be classified into the Na/Cl-type, Ca/SO_4-type and Na/SO_4-HCO_3-type. The neutral pH of the $CaSO_4$-type water could have been formed by local leaching of conductively heated ground water. (It should be noted that the area is extensively mineralized). The distribution of Na/Cl-type water is genrally localized inside and along the peripheral boundary of the young plugs, while the Ca/SO_4 type is distributed outside the plug. The whole geochemical model structure of the family of water in the area appears to be dome-like with the Na/Cl-type water occupying the lowermost zone; the Ca/SO_4-type, the uppermost zone; and the Na/SO_4-HCO_3 type occurring as a transition zone.

The origin of all hot spring waters could be attributed to meteoric water. The Na/Cl-type hot spring water shows positive oxygen shift while the O/H isotopic composition of the Ca/SO_4-type lies on the meteoric water line. Moreover, the localization of the Na/Cl-type water zone is controlled by the Balatoc and Itogon plugs. It is likewise controlled by the conjugate fracture system (northeast and northwest faults).

Fig. I–2–1 is a conceptual model of the Acupan-Itogon geothermal area which shows the hot thermal fluid ascending through permeable structures and reaching the surface along the peripheries of the Balatoc and Itogon plugs. It is, how-

ever, possible that the two dominant tongues of upflow zones would merge at some depth below the surface suggesting a single heat source located between the Balatoc and Itogon plugs. This, however, will have to be confirmed by deep drilling program to be undertaken in Phase-III of the Technical Arrangement.

3. MICROEARTHQUAKE SURVEY

3 MICROEARTHQUAKE SURVEY

3.1 Objective

Results of Phase-I geoscientific studies conducted in the project area show that highly prospective ground lies around the Balatoc and Itogon Plugs. Generally, the usual electrical methods of geophysical exploration which was applied in the second phase activity would have been able to infer the location of the reservoir. However, it turned out that the electrical noise caused by the underground mining activities within the project area had limited the capabilities of the methods employed. Thus, this lead to the adoption of a seismic monitoring system to record microearthquakes activities in the area that could be associated with geothermal reservoir behaviours related to fault movement, phase or load changes, etc.

There are numerous reports in locating reservoirs or heat source of geothermal fields in U.S. and Iceland which were delineated by this method. In Japan, it helps to define the boundary limits of the reservoirs in their known geothermal fields.

3.2 Introduction

3.2.1 Earthquakes and Seismic Waves

An earthquake is a sudden motion or trembling of the earth caused by the abrupt release of slowly accumulated strain (by faulting or by volcanic activity) through the generation of seismic waves. Seismic waves are generally elastic waves because they cause deformation of the material in which they propagate. The two types of seismic waves are body and surface waves.

Body waves are seismic waves transmitted in the interior of an elastic solid or fluid and not related to a boundary surface. Surface waves are seismic waves that propagate along the earth's surface.

The two types of body waves are primary (P-wave) and secondary (S-wave). The particle motion associated with P-wave is compressional (dilational wave) and is in the direction of the wave propagation, while that of S-wave is distortional (shear wave) and is perpendicular to the direction of propagation. The types of surface waves are Rayleigh, Love, channel and coupled waves.

The velocity of propagation of a P-wave (longitudinal wave) is faster than that of an S-wave (transverse wave) and a difference of arrival time between P- and S-waves occur at a certain point or station. This time difference is called the duration of preliminary tremors or simply S-P time. It is proportional to the hypocentral distance which is the distance between a hypocenter and a point or observation station. The time from the arrival of the P-wave to the end of an earthquake motion is known as the total duration of oscillation or F-P time.

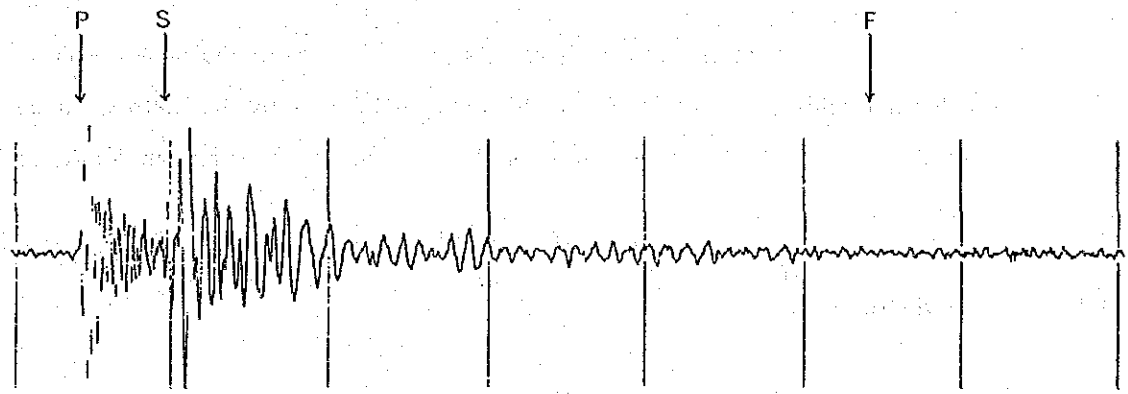

Fig. III–3–1 Seismogram

Earthquakes are also categorized as shallow-, intermediate- and deep-focus. The boundaries of their focal depths as suggested by B. Gutenberg and C. F. Richter (1949) are < 65, 65–300 and > 300 kilometers, respectively.

Shallow earthquakes (focus of less than 65 kilometers) sometime occur in succession within a short period. The normal process is that the biggest earthquake called the main shock is followed by a long sequence of aftershocks which may continue even for several years. In addition, the mainshocks may be preceded by small earthquakes, so called foreshocks. These are mostly so small that, as distinct

from the aftershocks, they are generally not recorded at distant stations.

A series of minor earthquakes, none of which may be classified as the main shock and occurring in a limited area and time, are called earthquake swarms. In these, all shocks are rather similar in magnitude and in general relatively small. The swarm starts with a few shocks, then their number gradually increases until a maximum is reached and then the whole phenomena dies out again gradually. In general, swarms are apt to occur in regions with present or earlier volcanic activity and may also be related to the movement of high temperature fluids. There is a good correlation, therefore, between the distribution of shallow earthquakes and volcanoes with high temperature zones that can be associated with geothermal resources.

A map showing the seismicity (magnitude, epicenter and period of observation of earthquakes) of an area is called a seismicity map.

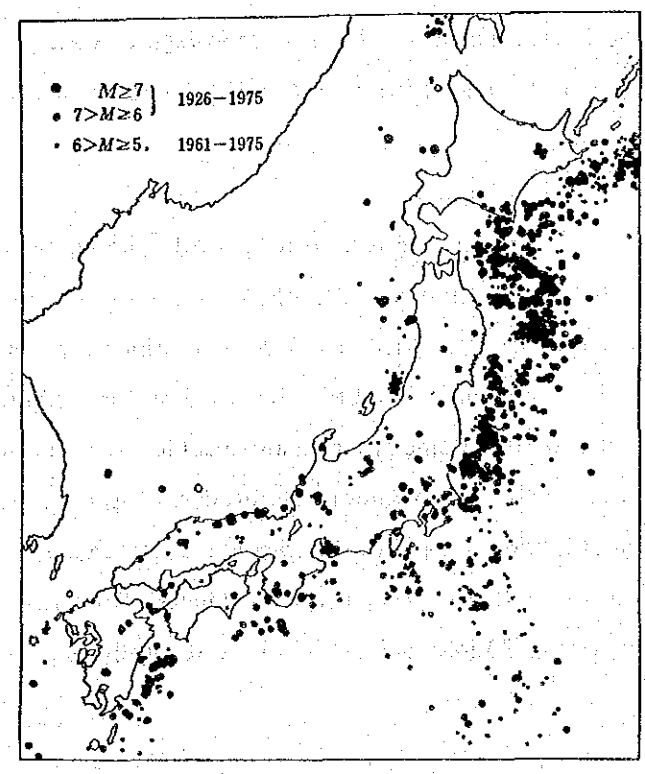

Fig. III–3–2 Seismicity Map

3.2.2 Hypocenter and Epicenter

An earthquake is associated with the destruction or rupture of rocks beneath the earth and the region where this occur is called the source region. The range of source regions are from 10 to 100 kms. and are represented by points called the earthquake focus or hypocenter. This is where the strain energy is first converted to elastic wave energy. The point on the earth's surface (longitude and latitude of the location) directly above the focus of an earthquake is called the epicenter. The distance between an epicenter and a station is called epicentral or angular distance.

3.2.3 Intensity and Magnitude

The value which indicates the strength of an earthquake motion and its effects at a particular place on man, on structures built by him and on the earth's surface is called intensity. The value is rated on the basis of a relative earthquake intensity scale system such as the Japan Meteorological Agency (JMA) Intensity Scale used in Japan which has eight (8) levels (0 to 7). Other such systems are the Mercalli, modified Mercalli and the Rossi-Forel scales.

The magnitude is used to quantify the characteristics of the total energy released by an earthquake. The Richter scale is used worldwide as the uniform measure of magnitude. C. F. Richter (1935) determined the standard scale by dividing in micron units the maximum amplitude recorded on the calibrated Wood-Anderson seismograph placed 100 kilometers from an epicenter. The magnitude is taken as the logarithmic scale of the said maximum amplitudes. However, the seismograph is not always placed 100 kilometers from the epicenter as stated above, so it was therefore revised to conform with varying epicentral distances. Each step of one magnitude in the scale represents a 10-fold increase in observed amplitude.

3.2.4 Passive Seismic Methods in Geothermal Exploration

Seismic methods used to explore or to monitor geothermal systems

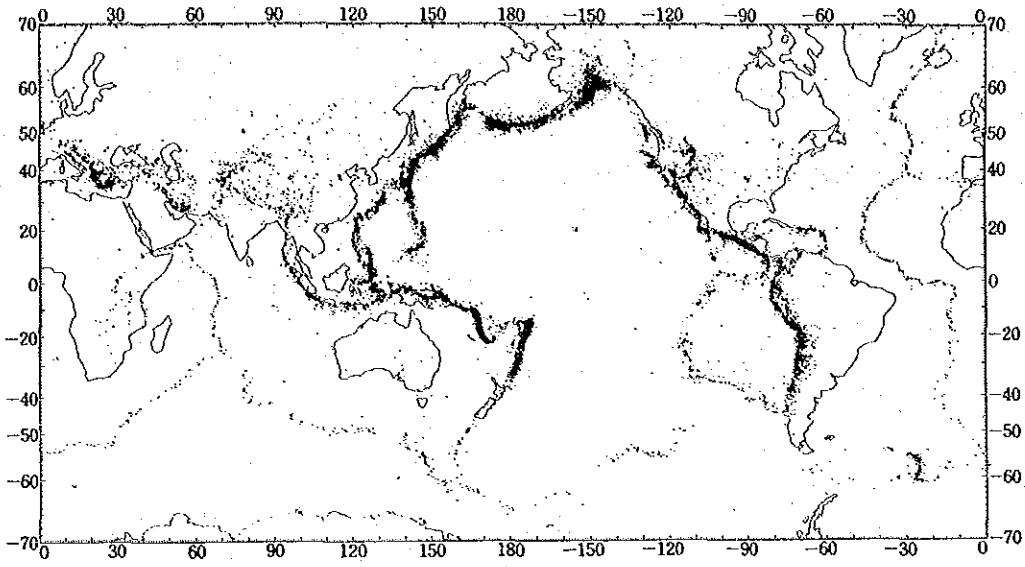

Depth: 10 ~ 100 km

Fig. Ⅲ-3-3 Seismicity Map in the World (d≦100Km, M≧4,1961~1967)

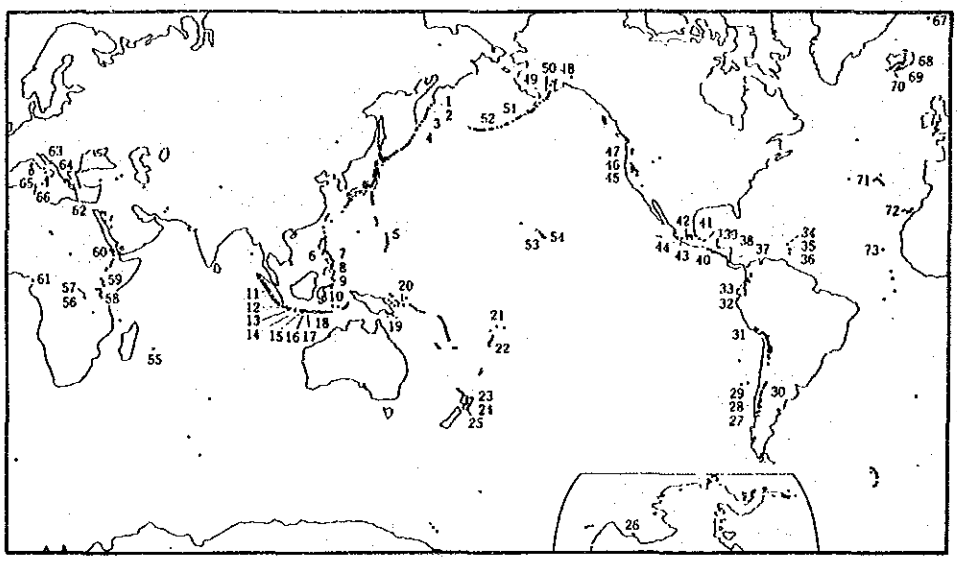

Fig. Ⅲ—3—4 Distribution of Volcanoes in the World

can be grouped into active and passive methods. Active methods such as refraction and reflection use artificial methods to produce or generate elastic waves, while passive methods rely on natural sources. These methods play important roles in interpreting seismic activities in geothermal areas such as in outlining the possible location and important features of the reservoir, and in relating seismic activities to geothermal systems. The passive methods usually employed are:

(a) Microearthquake survey: The term microearthquake is used to describe events of which magnitude are less than 3. Since geothermal areas occur in seismically active regions or margins, a certain microearthquake activity can be expected from these areas.

Results from this survey usually yield informations such as location of faults where geothermal fluid may pass, fractures, magma chambers and the influence of production and reinjection of hot water in a geothermal system.

Microearthquake observation has been carried out in numerous geothermal areas and results were reported to be successful. This does not necessarily mean, however, that it was the only method applied to pinpoint the location of geothermal resources.

(b) Teleseisms: An earthquake recorded by a seismograph at a great distance (over 1,000 kilometers) from the epicenter is called a teleseism. Teleseismic surveys give information about the crustal structure and subcrustal structure of heat sources. It is based on the phenomenon that the velocity and amplitude of seismic waves in the crust and upper mantle decreases significantly with temperature. The travel time of seismic rays which emerge with an angle of emergence of about 90°, that travel through the whole section of anomalously hot crustal rocks beneath a geothermal reservoir, is therefore delayed compared with the travel of the same event recorded away from the reservoir. The method is also called P-wave delays or P-wave attenuations due to the use of travel time delays of teleseismic events.

(c) Ground Noise Survey: In geothermal areas, certain ground movements which could be due to condensation or flashing of steam at shallow levels are likely to occur. This type of motion is called microseisms or ground noise. Results from this survey are in the form of maps showing average amplitudes for certain frequency bands or amplitude differences (in dB) with respect to quiet sites outside the prospect area.

3.2.5 Seismographs and Earthquake Observations

Even though earthquake observations were expressed quantitatively in an intensity scale, the purely descriptive reports employed in early times were far from the mathematical foundations of the elastic theory to permit unification of the two discripline. The development of seismographs to record earthquakes introduced exactness into seismology. The permanent continuous record of earth motion written by a seismograph is called a seismogram. A seismograph, whose physical constants are known sufficiently for calibration that the true ground motion can be calculated from the seismogram, is called a seismomenter.

Seismographs

A seismograph applies the pendulum principle in that it has some fixed points able to record the earthquake motion. This fixed point corresponds to the seismograph pendulum which has to be made more or less independent of its surrounding by special suspension. A typical seismograph assembly consists of a pendulum, a chronograph and a recording device which writes a line representing the motion of the pendulum on the chronograph drum.

There are three types of seismographs which differ by the manner in which the pendulum motion relative to its frame is transmitted to the record.

(a) Mechanical : The motion is transferred from the pendulum to the recording pens in a purely mechanical way and simultaneously magnified. In addition, the recording is mechanical (stylus on smoked paper).

(b) Optical : A mirror is attached to the pendulum or other parts

connected to it, and this reflects a light beam towards the photographic paper on a recording drum. This was developed due to the limitations of the mechanical type.

(c) Electromagnetic : Coverts the movements of a pendulum into electrical signals.

The other type of seismographs relative to the period of the pendulum with that of the periods of ground motion are:

(a) Displacement seismograph : If the pendulum period is much longer than the ground period, the deflections on the record are proportional to the displacement (in micron) of the ground.

(b) Velocity seismograph : When the periods of the pendulum and the ground are about equal, the deflections are proportional to the velocity (cm/sec. or kine) of the ground motion.

(c) Acceleration seismograph : If the pendulum period is much shorter than the ground period, the deflections are proportional to the ground acceleration (gal.).

The range of amplitude and frequency of an earthquake is very wide. A big earthquake can cause free oscillations on the earth for a period of about 10 minutes and can cause over-scaled recording even on seismographs with low magnifications. However, seismographs with greater than 10^6 magnifications are usually used for ultra-microearthquake observations where the predominant frequency of seismic waves is higher than 10Hz.

The selection of the right type of seismograph to be used in any observation will therefore depend upon the purpose and scope, magnitude and frequency of the earthquakes to be studied.

Seismograph Network

A pattern or configuration of seismograph statons, often so arranged as to provide a check on the consistency of the measured values is called seismograph

network or simply network.

Until the 1950's, the smoke paper recording system was commonly used in every network. The advanced development of electromagnetic seismographs made electrical recording by telemetry system possible. Earthquakes detected on all seismometers can now be received and recorded by a single multi-channel station (usually called the base station).

Recordings usually obtained from a network is voluminous compared with the desired recordings of earthquakes to be studied. The network should therefore be able to record in continuous form (paper) for on-spot monitoring and stored-form (magnetic tapes) for selective recording of actual earthquakes motions for easy processing. An equipment designed for selective recording called signal delay unit can be used, which is composed of:

(a) a signal memory unit or signal delay component capable of storing seismic wave signals for a given time; and

(b) a trigger unit which controls or triggers the selective recordings when an earthquake motion or signal is detected.

The equipment in conjunction with telemetry system is widely used at present and with the further development of digital recording, it is now possible to obtain immediate analyses of earthquake measurements through the use of modern computers.

3.3 Field Methodology

The network was established to cover a relatively wide area as possible since no previous earthquake observation was conducted over the project area. Earthquakes of magnitude 1 to 3 (microearthquakes) were mainly monitored.

3.3.1 Establishment of Stations

(a) Location of stations: Sites for the five (5) seismometers were selected on maps of 1:25,000 and 1:10,000 scales taking into consideration the following conditions:

(i) The stations should be 2 to 4 kilometers away from each other.

(ii) Radio telemetry was adopted instead of connecting the stations by cables into the base station. This is due to the very steep and rugged topography of the area.

(iii) The transmitters and receiver (base) station antennas should have complete or unobscured line-of-sights.

(iv) The Acupan and Itogon-Suyoc Mines are almost in the center of the network and are being operated continuously. These mines could generate artificial seismic waves and cause constant ground motions from their mining activities. Therefore, the locations of the stations had to be chosen so that not all of them should be influenced by the said artificial waves at the same time. This will leave some stations for cross-checks on the nature of the wave.

(v) The stations should also be far from populated places and busy traffic which would cause unnecessary ground noise.

(vi) Stations should be accessible considering the power supply batteries for the transmitters have to be changed two to four days.

(b) Noise monitoring: The ground noise were measured near the planned site of the stations by the system shown in Fig. III–3–5.

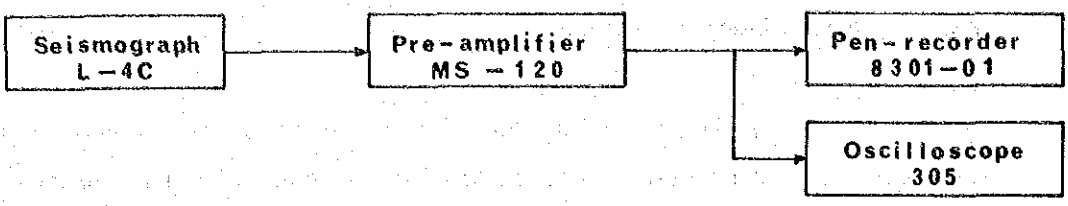

Fig. III–3–5 Noise Measuring System

The amplitude of the microseism A (in kine) is calculated from the following equation:

$$A = (a/t)10^{-n} \qquad \text{------ (1)}$$

where a is measured using a pen recorder or oscilloscope (volt),

10^n, amplification factor,

t, in V/kine, is the magnification of the seismometer.

The locations were selected from points with the lowest noise levels. The seismograph response from radio telemetry signal was then tested before actual orientations for both transmitter and receiver antennas were finalized.

(c) Setting of Seismograph: A hole about one meter is both diameter and depth is dug to emplace the seismometer. The bottom of the hole is reinforced with iron rods before being cemented. If the bottom is not hard or compact enough, a thin hole about 50-cms. deep is drilled using a 10-cm. diameter bit before cement is poured.

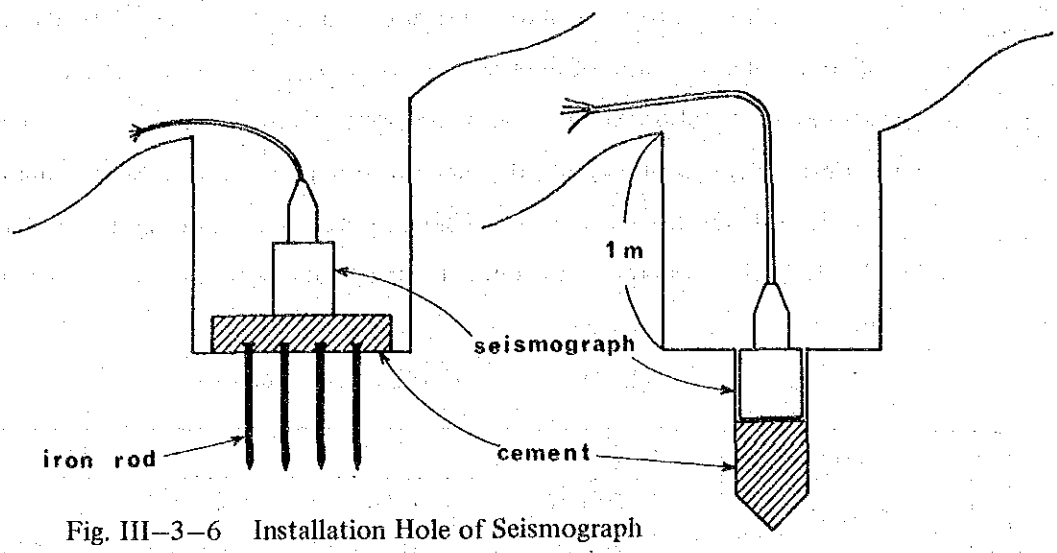

Fig. III–3–6 Installation Hole of Seismograph

The seismograph is then covered with soil after having been properly set and levelled horizontally and vertically. The three-dimensional seismometer (L4C-3D) must also be properly oriented to the north-south and east-west direction to measure horizontal ground movement. The cable from the seismometer to the transmitter is likewise buried to the ground to protect it from people and animals. The transmitter and batteries are then placed inside a specially constructed dog-house-like box. The area is fenced with barbed wires with the box and antenna inside. A typical station set-up is shown in Fig. III–3–7.

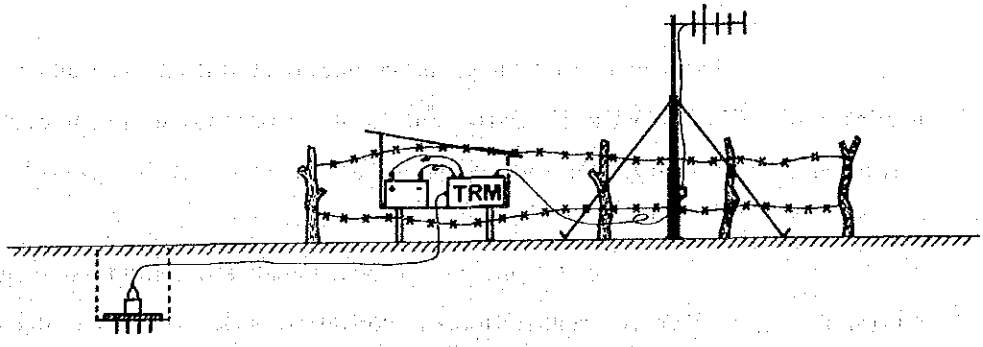

Fig. III–3–7 Seismographical Station

(d) Survey of Station Location : In order to accurately determine the epicenter and hypocenter of microearthquakes to be studied, the exact locations of the seismograph stations should also be precisely measured. The BED team conducted the topographic survey for the locations of the seismic stations using triangulation and stadia-traverse methods. The results are shown in Fig. III–3–8 and Table III–3–1. These were based from benchmarks and coordinates of Benguet Corporation.

Table III–3–1 Coordinates of Network

No.	LATITUDE	LONGITUDE	X	Y	ELEVATION(m)
1	16°21.18'N	120°39.91'E	763.66E	5,647.77S	1,246.83
2	16°22.48'N	120°40.03'E	1,003.14E	3,226.54S	986.87
3	16°21.74'N	120°40.98'E	2,703.25E	4,628.85S	835.66
4	16°20.03'N	120°39.95'E	836.71E	7,828.71S	1,508.61
5	16°21.25'N	120°38.45'E	1,837.41W	5,385.78S	1,249.87

3.3.2 Method of Observation

Five (5) seismometers were utilized during the survey. One is three-dimensional (type L4C-3D) to simultaneously measure the horizontal (north-south and east-west) and vertical ground movements while the other four are vertical seismometers (type L4C). The locations of the seismometers are shown in Fig. III–3–9. The seismic recording system is shown in Fig. III–3–10 and equipment specifications are described in Table III–3–2.

The signals from the seismographs are amplified and transmitted by wireless radio (FM) using the 400 MHz band to the receiving base station at Baguio Townhouse, Baguio City. It is about 9 kilometers northwest of the network.

At the base station, the received signals are demodulated by the corresponding receivers for each station and converted back into electric signals. These are then reproduced by the pen recorders into the paper chart with the corresponding time code for continuous recording and monitoring.

For selective recording when seismic movement occur, the signal delay equipment is automatically set for use aside from the paper chart. This happens when the received seismic signals from any three of the five seismographs stations are higher than the trigger level pre-set for the system. The trigger unit of the equipment sends a command that will release the data recorder from the "pause" to "record" state. Simultaneously, the signal memory unit converts the seismic signals to 8-bit digital data and stored into a 4-kilobyte IC memory. The data is stored for 8 seconds before being transformed back by the digital-to-analog (D/A) coverter into analog or electric signals. Finally, the seismic data is stored into the magnetic tape data recorder.

Noise monitoring was started on October 8, 1983 and the seismograph locations were finally selected by October 14. The setting-up of seismograph and base stations was carried out from October 10 to October 17.

Microearthquake observation was conducted for a period of 55 days from October 14 to December 7. During the entire survey, the gains of the telemeters (transmitters and receivers) were set at 60 dB. 450-meter long charts were used and the speed was set at 5 mm/sec for the pen recorders. The trigger level of the signal delay unit is from 200 to 700 mV amplitude.

The recording time lasts for about 70 seconds before it automatically stops. The resolution of the monitoring system is about 10 micro-kine. The lowest magnitude (M) of ultra microearthquake it can record is bigger than one (1) when hypocentral distance is less than 20 kilometers and bigger than 0 when it is less than 5 kilometers.

SMF 12 Vdc batteries (70 A.H.) were used for the power supply of each seismograph station which were changed and recharged every two to four days.

The recorded seismic signals are timed with reference to the clock marks on the seismograms. Standard time is calibrated by comparing the marking clock with the radio time signals (10 MHz band) from JJY or BPV, which are the coordinated universal time. The former is sent from Tokyo, Japan and the latter from Shanghai, People's Republic of China.

Occurrences of microearthquakes and equipment troubles were determined from the monitoring pen recorders. Problems such as the bad condition of transmitters, breakdown of cables by animals and loss of battery power briefly interrupted the recordings in some stations. Otherwise, recording had been continuously executed without interference except when changing the batteries. Although weather disturbances which include three typhoons hit the area in October, these did not damage the towering antennas of the stations nor interrupted the recordings.

3.4 Analyses of Data

The network is generally set to detect microearthquakes or seismic waves of less than 100 mV amplitudes or about 40 micro kine. The lowest magnitude of microearthquakes that the network can detect is 1.0 based from Watanabe's equation for computing magnitudes. This could be detected as far as 40 kilometers from the station.

Since diorites and granodiorites are widely distributed in the area, the general velocity of the primary (Vp) and secondary (Vs) waves were refered for these rocks. Then, Omori's coefficient of about 8 kms/sec. was adopted. In this case, the detection limit for microearthquakes is S-P time of about 5 seconds or less. Only events with S-P times of 5 seconds and below were therefore analyzed.

3.4.1 Seismic Records

Seismic signal are immediately examined from each of the 450-meter paper charts after been used up by the pen recorders. At 5 mm/sec. speed, the chart is used-up and replaced everyday. Only those parts with significant seismic wave signals were extracted from the seismograms. When the records have been obtained, the arrival times, periods, phases and amplitudes of the seismic wave are then determined. These were arranged according to the time of occurrence in the form of tables. The gain setting for each station, which is the trigger level setting for aach station at the signal delay unit, were then noted.

The tables were used as references in future analyses of data stored

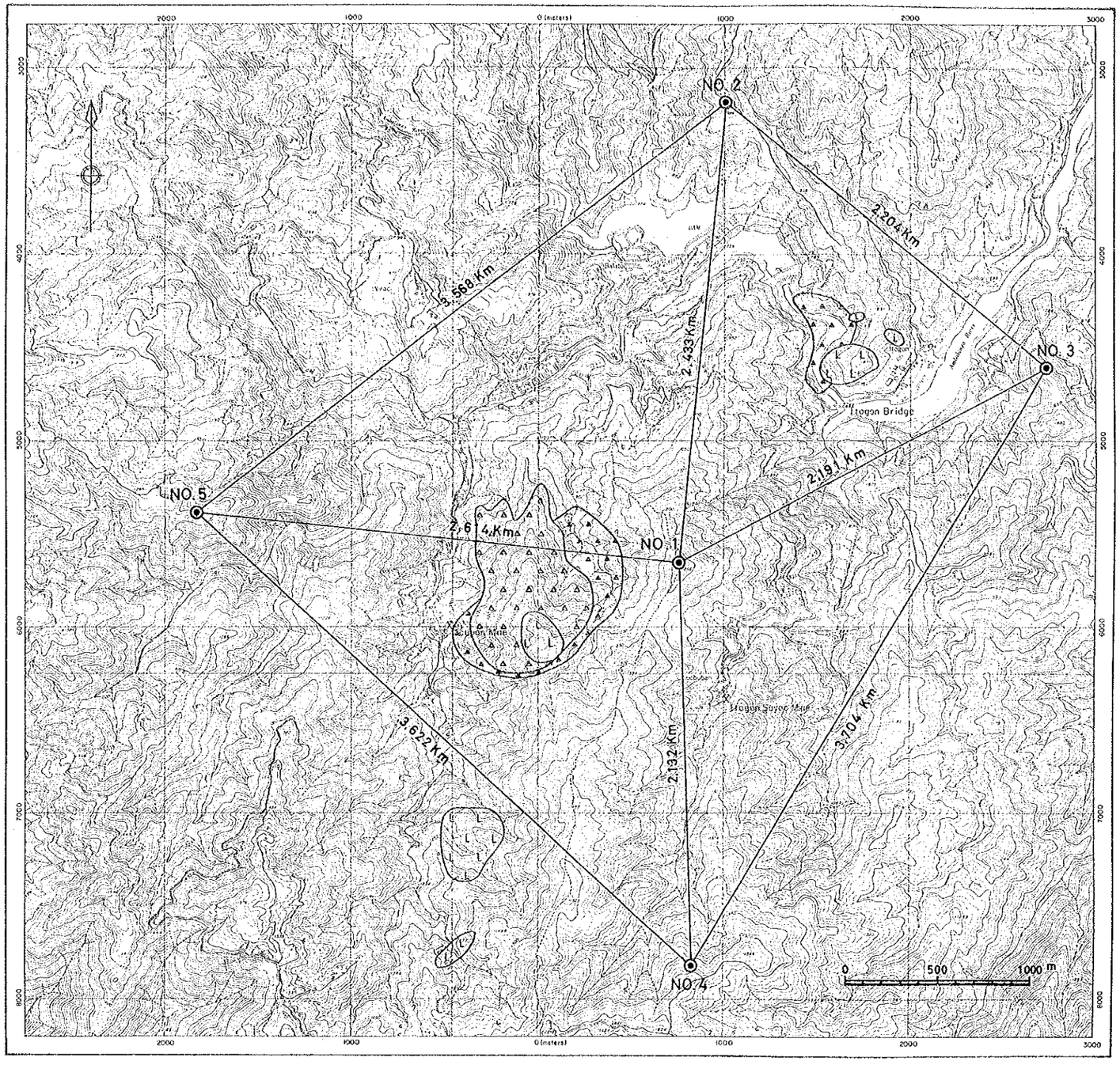

Fig. Ⅲ-3-8 Location of Network

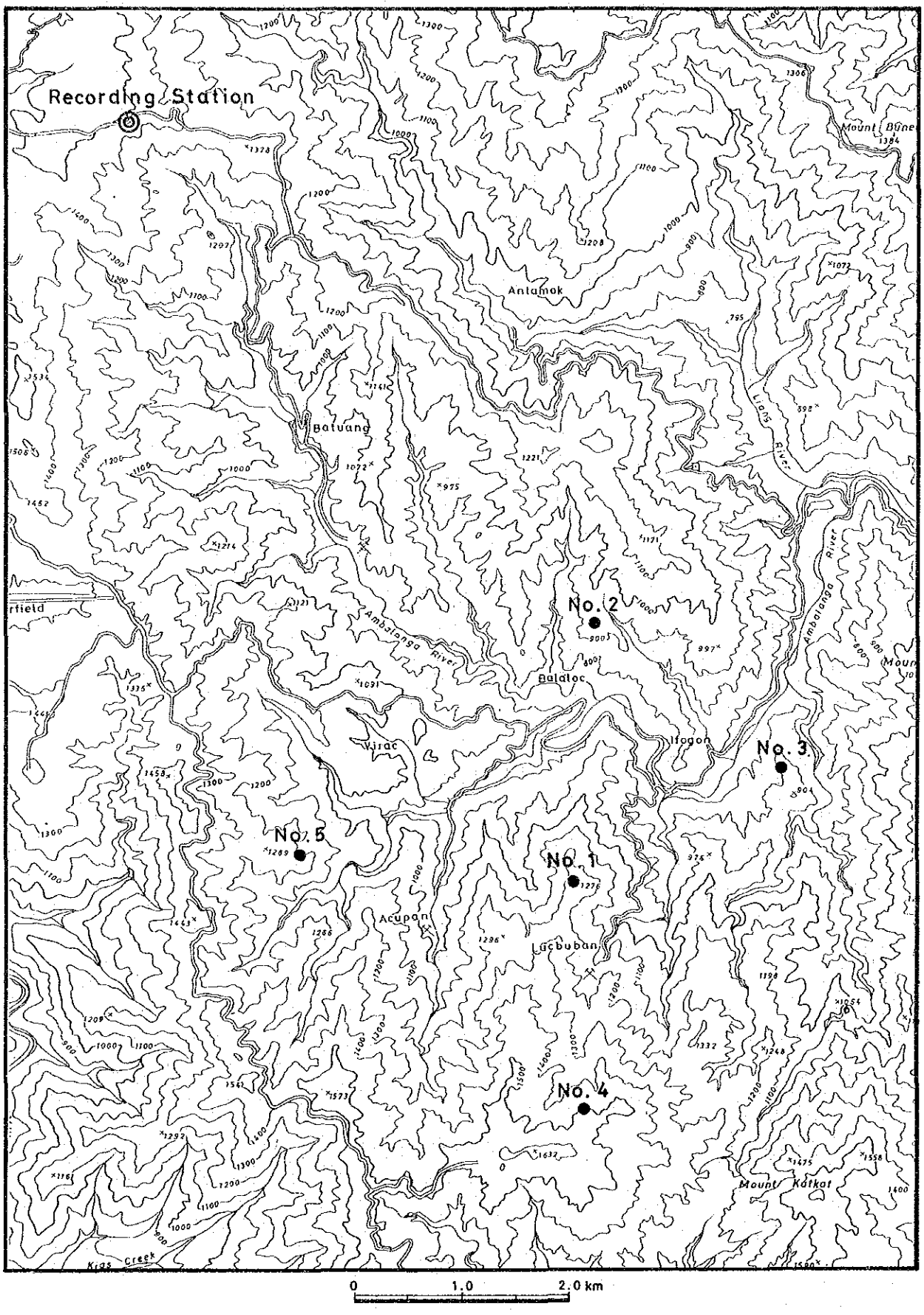

Fig. Ⅲ-3-9 Location Map of Seismographs

Table Ⅲ-3-2 Specification of Recording System

Instrument	Manufacturer	Model	Q'ty	Specification
Seismograph	Mark Products	L-4C-3D	1	3-component, Natural frequency 1.0 Hz, Coil resistance 5,500 Ω, Transduction 2.76 V/kine (open)
		L-4C	5	Vertical component, Natural frequency 1.0 Hz, Coil resistance 5,500 Ω, Transduction 2.76 V/kine (open)
Amplifier	Chiba Denshi Labo., JAPAN	MS-120	1	Frequency Response DC ~ 50 Hz flat, Gain 0, 20, 40, 60, 80 dB, 1ch
		MS-140	2	Frequency Response DC ~ 50 Hz flat, Gain –20, 0, 20 dB, 3ch
Radio-Telemeter	Meisei Electric Co., Ltd., JAPAN	TRM-812	6	4ch, Gain 0 ~ 60 dB 6 dB step, Frequency Response DC ~ 30 Hz flat, Frequency Modulation 400 Hz, Power 1W
		RCV-812	6	4ch, Sensitivity 3mV ~ 3V rms, 400 Hz, Receiving sensitivity less than 1 μV
Pen Recorder	NEC-Sanei Instrument Co., Ltd., JAPAN	8K23-1L	1	8ch, Heat Pen, DC ~ 80 Hz, Maximum sensitivity 0.5 mV/cm, Chart speed 1 mm/min ~ 100 mm/sec,
		8K13-1L	1	8ch, Heat Pen, DC ~ 80 Hz, Maximum sensitivity 0.5 mV/cm, Chart speed 1 mm/min ~ 100 mm/sec
	Hioki E.E. Co., JAPAN	8301-01	1	1ch, Heat Pen, DC ~ 100 Hz, Maximum sensitivity 2.5 mV/cm, Chart speed 1 ~ 25 mm/sec
Data Recorder	Sony Magnescale Inc., JAPAN	FE39-A	1	8ch, EL cassette tape, DC ~ 1 kHz, Analog FM, Tape speed 3.8, 9.5, 19 cm/sec
Signal Delay	Sanei Instrument Co., Ltd., JAPAN	9A08	1	Signal Delay Unit 8ch, 8 bits, 4 k word IC Memory, Delay time 8 sec, DC ~ 50 Hz, Sampling 100 Hz
				Trigger Unit Trigger level ± 50 ~ ± 500 mV, 10ch, Trigger mode 3/4/5 ch AND/ON
Time Code Generator	Citizen Corp., JAPAN	8621A-43	1	Digital Quartz Clock 8.192 Hz, Output BCD, 1 Hz Busy, 12 hours, 1 hour, 1 min., 1 sec Pulse, TTL, etc., Deviation 0.05 sec/day
Oscilloscope	Sony Tectronix Co., JAPAN	305		Frequency DC ~ 5 MHz, sensitivity 5 mV/div ~ 10 V/div
JJY Receiver	Sony Co., JAPAN	ICF-2001	1	Receiving Frequency AM 150 ~ 29999 Hz FM 76 ~ 108 Hz

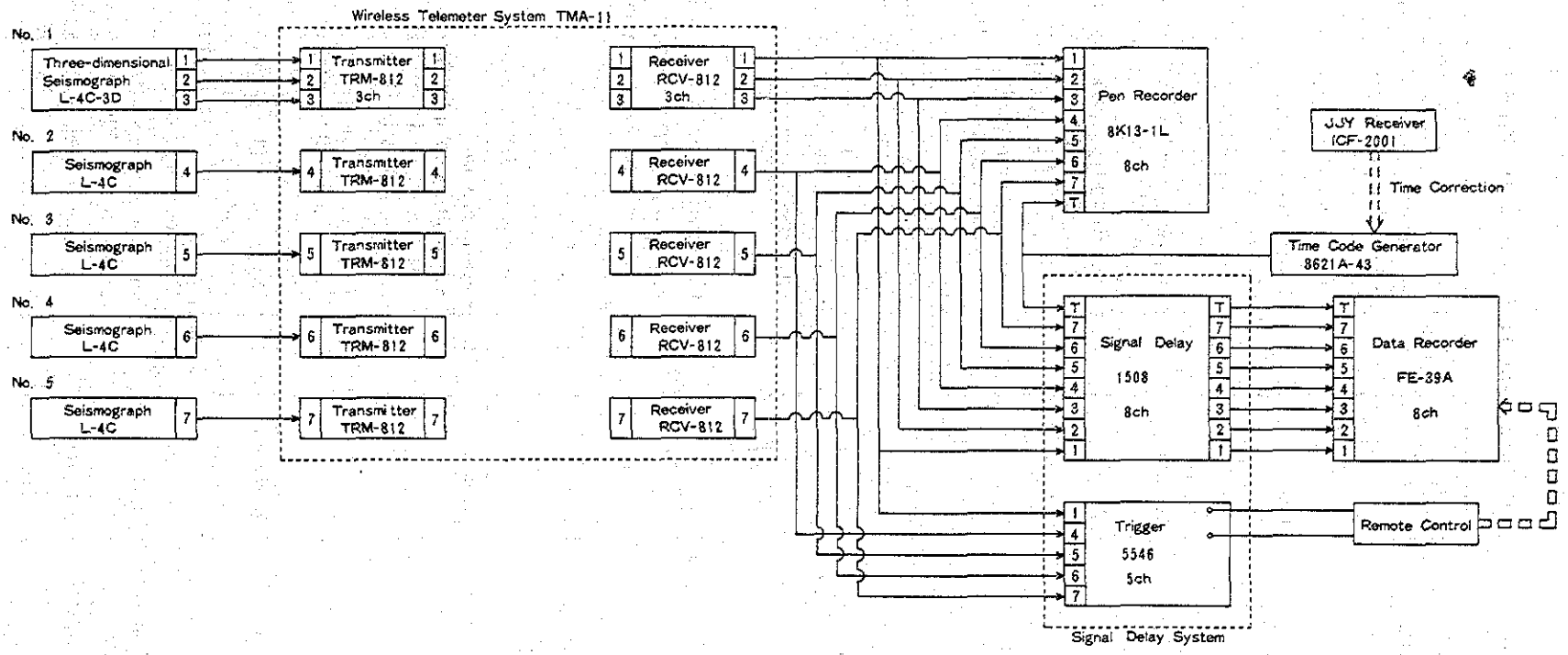

Fig. Ⅲ-3-10 Recording System

in the magnetic tape recorder. These selected recordings are then reproduced by pen recorders at speeds of 1, 5 and 10 mm/sec. Replays of the recordings at 5 mm/sec. are available at the BED office. Data were likewise stored into computers where they were revised to Philippine standard times after corrections were applied to the corresponding pen recorders. The magnitudes were likewise computed and results were placed in table forms. Events which were not recorded on tape were taken from the paper charts and were likewise processed and added to the tables.

3.4.2 Hypocenter Determination

When an earthquake focus that lies relatively close to the network is detected on only a few stations, the idea of a flat and homogenous earth is generally assumed. Therefore, the focus (Xo, Yo, Zo) can be calculated from the equation.

$$(Xi-Xo)^2 + (Yi-Yo)^2 = Vp^2\ (ti-to)^2 \qquad \text{------ (2)}$$

where: (Xi, Yi, Zi) are the coordinates of the station

ti, the arrival time of P-wave

to, origin time and the instant at which the earthquake event started at the hypocenter

Vp, is the velocity of the P-wave.

Depending on the available measurable quantities from the recordings, the following methods can be used in determining the focus:

(a) Method using S-P times from three (3) stations: The S-P arrival time (tspi) is proportional to the hypocentral distance (Ri) as expressed in the equation

$$Ri = k\ (tspi) \qquad \text{------- (3)}$$

The value of k varies for different areas, and is generally from 4 to 9 kms/sec. Combining equations (2) and (3), we get the following Omori's formula for hypocentral distance:

$$(Xi-Xo)^2 + (Yi-Yo)^2 = k^2\ (tspi)^2 \qquad \text{------ (5)}$$

We can therefore determine the focal coordinates of an earthquake from the S-P arrival times from three stations.

The value of k can also be determined using Poisson's ratio. This is the ratio of the fractional transverse contraction of the fractional longitudinal extension of a body under tensile stress. However, if the Vp and Vs for the area is unknown, the general value ¼ of Poisson's ratio is used.

(b) Method using S-P times from four (4) stations: This method is used when the value of k is unknown. The S-P time arrival from four stations are needed to determine the focal coordinates.

(c) Method using S-P and P-wave arrival times: If the Poisson's ratio remains constant, the relation between the S-P and P-wave arrival times obtained from a station, will be linear, even if we assume the earth to be non-homogenous. This relation is shown in the figure called Wadachi's diagram. Since the S-P interval at the focus is equal to 0, the origin time (to), can be obtained from the point where the straight line crosses the line of S-P time = 0 on the Wadachi's diagram. The hypocentral distance (Ri) can then be calculated from the following formula if Vp is known:

$$Ri = Vp\ (ti - to) \qquad \text{------ (6)}$$

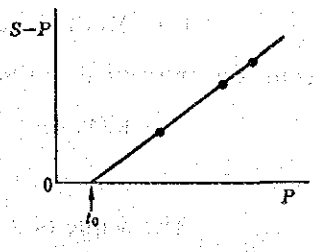

Fig. III–3–11 Wadachi Diagram

Once the hypocentral distance from three stations are determined, the focus can be calculated from method (a).

(d) Method using P-wave arrival times: In cases where data can be obtained from three stations, Omori's formula is suitable in calculating the hypocenter. However, Poisson's ratio is usually unknown and equation (2) is used with the value of Vp and the arrival times of P-wave from four stations.

(e) Method using P and S travel time curve: In this method, the velocity structures for P and S wave are assumed from drawn travel time diagrams. Using P-arrival and/or S-P interval times, a technique similar to the use of graphs is adopted manually and through the aid of computers.

(f) Least Square Method: When the longitude, latitude, depth and time of occurrence of the hypothetical focus is given as X, Y, h and t, respectively and if the true focus is given by X + dX, Y + dY, h + dh and t + dt; the values of dh and dt are obtained by the least square method. If the observed travel time at a certain station from the hypothetical focus is Oi, and the theoretical travel time is Ci, the normal equation for the least square method is:

$$\frac{\partial Ci}{\partial \Delta i}\frac{\partial \Delta i}{\partial X}\,dx + \frac{\partial Ci}{\partial \Delta i}\frac{\partial \Delta i}{\partial Y}\,dy + \frac{\partial Ci}{\partial h}\,dh + dt = Ci - Oi \qquad \text{------ (7)}$$

where: $Oi = ti - t$

$\Delta i =$ epicentral distance obtained from the table of standard travel times.

Also, if the azimuth of the station (i) as seen from the epicenter is θi, then

$$\partial \Delta i/\partial X = \sin\theta i \cos Y \qquad \text{-------- (8)}$$

$$\partial \Delta i/\partial Y = \cos\theta i \qquad \text{-------- (9)}$$

Using equations (7) to (9), the values of dX, dY, dh and dt can be calculated and are added to X, Y, h and t, respectively, to get the new hypothetical

focus. The procedure is repeated over and over until dX, dY, dh and dt satisfy the given conditions. This is known as Geiger's method. It is usually applied in cases with ten or more stations. However, it was revised, taking the advantages of methods (1), (2), and (3) mentioned earlier. The quality of the observed data was further improved by re-reading the records, nothing the various differences in errors in calculating the focus.

3.4.3 Magnitude Determination

There are various methods for estimating an earthquake's magnitude based from Richter's definition. The methods should take into consideration the type and characteristic of the seismograph to be used and should be designed to conform to the standard magnitudes of the main earthquakes in the world as established by Gutenberg (1949) and Richter (1954).

The magnitudes of the earthquakes observed in this survey were determined by methods adopted for the characteristic of the seismograph used.

(a) Tsumura's method: Tsumura (1967) noticed that the period of an earthquake is exponentially proportional to the magnitude, and expressed this in an equation for epicentral distances of less than 200 kilometers.

$$M_T = -2.36 + 2.85 \log Td \qquad \text{------ (10)}$$

where: M_T is Tsumura's magnitude
Td in seconds is the duration or period of the tremor.

As can be seen from the equation, the magnitude can be approximated even when the epicentral distance or the amplitude of an earthquake is unknown.

(b) Watanabe's Method: This method was devised to determine M from the amplitude of the maximum velocity Av (kine) and from the hypocentral distance r (km). Similar equations were formulated by other seismologists like Mura-

matsu (1964), Terashima (1968), and Watanabe (1971). For this survey, Watanabe's equation was used.

$$0.85\ Mw = 1.73 \log r + \log Av + 2.50 \quad \text{------ (11)}$$

where Mw is the magnitude from Watanabe's equation.

From this equation, the magnitude can be calculated when the focus has been earlier determined as long as the record's amplutude are not over-scaled. In Tsumura's equation (10) the magnitude cannot be determined for cases where the noise level is too large, or there are overlapping of seismic signals from other earthquakes.

Results from microearthquake surveys conducted in Japan show good correlation between M_T and M_W and only earthquakes whose magnitudes can be determined from M_T or M_W were analyzed for this survey.

3.5 Evaluation of Results

Nine hundred seventy three (973) earthquake occurrences were recorded during the 55-day survey conducted from October 14 to December 17, inclusive, among which two hundred thirteen (213) were classified as microearthquake ($M < 3$).

From these records, the arrival times of various phases, periods and amplitudes for the different waves are taken. The data are then processed by the electronic computer system described in Table III–3–3.

Table III–3–3 Data Processing System

Instrument	Maker	Model	Specification
Desk Top Computer	Hewlett Packard Inc.	HP9845B	187 Kbyte RAM, addition 270 μsec
		HP9826S	832 Kbyte RAM, addition 137 μsec
Graphics Printer		HP2631G	7x9 dot matrix, 132 Char./Line
		HP2671G	7x9 dot matrix, 80 Char./Line
Flexible Disk Drive		HP9885M	1 drive, 0.51 Mbyte
		HP9895A	2 drive, 2.36 Mbyte
Graphics Plotter		HP7580A	8 pen, size A4 ~ A1, 25μ
Graphics Tablette		HP9111A	reading 60 point/sec, 0.1 mm

All the recorded earthquakes during the survey are shown in the table of appendix while data on microearthquakes (S-P times of 5 seconds and below) are described on the Table in Appendix.

3.5.1 Daily Frequency Diagram

Daily earthquake occurrences were summarized and shown in Fig. III–3–12. The diagram shows November 16 with the highest number of occurrences recorded in a single day. December 5 has the lowest after disregarding October 14 and December 8 since the recording time during these days were shorter due to battery troubles. The average rate is about 18 events per day.

Earthquakes with 5 seconds or less S-P times occurred at about four per day. There were no earthquake swarms observed during the entrei period as can be seen from the diagrams.

3.5.2 Histograms by S-P times

Two histograms were made for occurrences with S-P times of less or equal than 30 and 5 seconds as shown in Fig. III–3–13.

Table Ⅲ-3-4 List of Hypocenters (1)-(5)

(1)

No.	Eq. No.	Time of Commencement	Hypocentral Coordinate			Magnitude	
			Lat.	Lon.	Depth	Tsumura	Watanabe
1	6	1983 10 15 12 21				1.07	1.16
2	11	1983 10 15 17 23				0.57	1.37
3	15	1983 10 15 22 29				-0.64	1.08
4	17	1983 10 16 0 31				-0.08	0.99
5	19	1983 10 16 1 8				1.12	2.34
6	24	1983 10 16 5 29				1.21	2.23
7	25	1983 10 16 7 31				2.70	2.68
8	29	1983 10 16 14 20				-1.23	0.78
9	31	1983 10 16 15 2				1.04	2.09
10	32	1983 10 16 16 29 41.28	15 59.38	120 29.94	18.96	1.11	1.78
11	33	1983 10 16 17 40				1.11	1.36
12	36	1983 10 16 22 46 36.03	16 27.04	120 35.37	40.67	0.82	1.50
13	41	1983 10 17 3 42 50.22	16 21.84	120 54.63	27.42	1.97	2.37
14	53	1983 10 17 7 43 9.25	16 26.41	120 43.52	3.65	-0.63	0.99
15	54	1983 10 17 8 27 35.93	16 24.55	120 50.92	19.79	0.09	1.31
16	62	1983 10 18 3 10 28.65	16 30.12	120 28.20	30.31	0.20	1.44
17	63	1983 10 18 3 44 25.86	16 32.18	120 32.10	26.29	1.41	2.28
18	64	1983 10 18 4 19 28.61	16 25.55	120 41.69	10.31	-0.38	1.45
19	67	1983 10 18 12 16 37.73	16 21.35	120 33.51	21.99	0.50	1.89
20	73	1983 10 19 1 27 21.83	16 35.27	120 32.00	20.31	1.35	1.82
21	74	1983 10 19 1 38 36.35	16 41.15	120 38.55	16.54	0.92	1.44
22	77	1983 10 19 2 52 55.79	16 35.40	120 29.44	11.96	0.60	1.40
23	81	1983 10 19 11 58 41.38	16 32.01	120 30.49	25.49	1.14	2.15
24	82	1983 10 19 13 10 41.98	16 28.52	120 51.17	24.21	0.72	1.74
25	86	1983 10 19 21 26 24.94	16 23.19	120 24.49	30.31	2.28	2.30
26	93	1983 10 20 1 34 41.34	16 21.72	120 27.66	21.95	0.59	1.74
27	94	1983 10 20 2 12 23.12	16 18.67	120 25.46	29.67	0.71	1.26
28	98	1983 10 20 14 45 46.86	16 8.47	120 31.97	28.38	1.62	2.19
29	99	1983 10 20 14 46 10.04	16 7.44	120 29.70	10.61	1.17	2.07
30	106	1983 10 20 20 50 11.56	16 21.28	120 40.01	46.98	2.03	1.63
31	116	1983 10 21 5 21 21.01	16 21.28	120 40.01	32.39	1.78	1.64
32	125	1983 10 21 20 9 7.38	16 21.35	120 22.85	26.46	0.84	2.10
33	132	1983 10 22 11 35 59.11	16 28.35	120 43.50	2.67	-0.82	0.87
34	134	1983 10 22 15 50 42.39	16 5.21	120 30.92	27.76	0.90	2.21
35	135	1983 10 22 15 52 15.28	16 9.31	120 33.09	28.70	1.24	1.81
36	136	1983 10 22 23 5 42.13	16 24.70	120 25.61	31.35	1.98	2.34
37	137	1983 10 22 23 15 50.97	16 21.35	120 21.78	34.80	0.91	2.35
38	138	1983 10 23 1 42 20.98	16 28.43	120 38.55	18.65	0.23	1.32
39	141	1983 10 23 2 47 43.15	16 25.41	120 40.76	5.26	0.49	1.35
40	147	1983 10 23 7 46 40.50	16 15.58	120 24.18	32.31	1.25	2.15
41	151	1983 10 23 11 27 53.49	16 26.74	120 32.91	15.18	-0.22	1.33
42	166	1983 10 23 23 42 23.96	16 25.12	120 52.81	26.13	1.17	1.88
43	167	1983 10 23 23 59 17.57	16 15.81	120 27.83	27.10	0.33	1.42
44	169	1983 10 24 1 27 36.43	16 17.64	120 24.73	31.27	1.48	2.21
45	177	1983 10 24 14 47 16.97	16 7.75	120 34.27	23.76	1.62	1.99
46	178	1983 10 24 14 47 3.76	16 9.21	120 33.23	27.90	1.15	1.79
47	179	1983 10 24 17 48 15.66	16 27.74	120 55.62	34.32	0.84	2.09
48	181	1983 10 24 18 58 50.81	16 20.13	120 40.05	34.48	0.94	1.49
49	182	1983 10 24 20 17 27.35	16 21.35	120 38.55	27.26	0.58	1.60
50	183	1983 10 24 21 33 30.26	16 24.79	120 23.44	33.52	1.47	2.00

No.	Eq. No.	Time of Commencement	Hypocentral Coordinate			Magnitude	
			Lat.	Lon.	Depth	Tsumura	Watanabe
51	184	1983 10 24 22 17 24.87	16 32.97	120 33.71	29.67	0.13	1.40
52	185	1983 10 24 22 33 30.76	16 41.73	120 41.08	35.28	2.78	1.64
53	192	1983 10 25 6 23 46.10	16 5.63	120 43.80	32.39	1.30	2.14
54	199	1983 10 25 11 26 7.00	16 14.03	120 35.58	18.89	1.24	1.61
55	204	1983 10 25 19 8 0.99	16 11.70	120 40.05	25.14	2.19	2.30
56	215	1983 10 26 5 16 9.27	16 36.32	120 35.23	32.72	0.78	1.53
57	223	1983 10 26 22 7 42.85	16 20.13	120 40.05	21.15	-0.07	1.23
58	233	1983 10 27 4 52 46.52	16 20.13	120 38.83	5.27	-1.07	0.31
59	247	1983 10 27 17 16 57.29	16 7.02	120 31.44	19.39	1.17	1.92
60	248	1983 10 27 17 16 20.64	16 9.32	120 33.07	27.74	2.31	2.21
61	255	1983 10 28 2 47 48.62	16 13.04	120 24.33	34.80	0.95	1.80
62	263	1983 10 28 19 4				0.41	1.54
63	265	1983 10 28 20 2 39.03	16 29.22	120 34.79	20.18	0.49	1.24
64	266	1983 10 28 21 54 35.63	16 27.35	120 29.01	13.25	1.46	2.10
65	280	1983 10 29 15 4 6.25	16 33.10	120 33.06	31.91	1.25	1.99
66	282	1983 10 29 17 58 56.96	16 25.81	120 23.84	30.23	1.71	2.53
67	308	1983 10 31 10 1 16.43	16 21.35	120 38.55	29.99	1.34	2.00
68	318	1983 10 31 22 24 50.13	16 20.13	120 40.05	26.70	-0.32	1.14
69	338	1983 11 1 20 24				0.71	1.67
70	341	1983 11 1 21 10 55.65	16 27.67	120 53.43	28.22	1.68	1.52
71	343	1983 11 2 1 6 42.25	16 21.35	120 20.93	36.40	2.71	2.57
72	344	1983 11 2 3 32 34.42	16 21.35	120 20.70	35.31	1.41	2.15
73	352	1983 11 2 12 9 31.98	16 30.97	120 30.45	0.84	1.94	2.24
74	353	1983 11 2 12 27 52.02	16 30.24	120 36.16	17.44	1.51	2.03
75	356	1983 11 2 14 22				1.33	1.65
76	357	1983 11 2 14 36 54.49	16 27.29	120 40.13	11.87	0.70	1.79
77	359	1983 11 2 16 6				0.18	0.85
78	360	1983 11 2 23 14				0.90	1.48
79	361	1983 11 2 23 27				-0.20	0.80
80	363	1983 11 3 1 20 58.95	16 28.34	120 38.55	17.28	0.20	1.20
81	365	1983 11 3 1 56 26.53	16 37.52	120 46.53	35.12	2.52	2.75
82	366	1983 11 3 2 24 40.00	16 42.94	120 38.55	37.05	1.13	2.00
83	369	1983 11 3 5 51 51.89	16 23.69	120 36.33	8.64	-0.20	0.45
84	375	1983 11 3 15 49 34.86	16 28.21	120 26.18	9.82	1.11	1.80
85	381	1983 11 3 21 53 42.92	16 26.30	120 40.41	2.72	0.67	1.52
86	384	1983 11 3 23 54 39.49	16 21.71	120 40.01	3.72	-1.74	0.53
87	391	1983 11 4 11 6 12.33	16 7.22	120 29.75	18.38	1.60	2.07
88	393	1983 11 4 13 9 7.51	16 29.22	120 42.77	4.57	0.05	1.49
89	395	1983 11 4 15 18 44.14	16 30.55	120 43.65	8.75	0.38	1.38
90	401	1983 11 5 5 26 25.34	16 27.65	120 56.53	34.16	0.97	1.79
91	407	1983 11 5 11 42				0.72	1.39
92	408	1983 11 5 12 50 53.73	16 24.97	120 29.41	23.08	1.79	2.17
93	411	1983 11 5 16 26 45.59	16 25.07	120 41.32	4.37	-0.25	1.62
94	424	1983 11 6 21 37 3.38	16 30.41	120 54.17	10.62	0.77	1.87
95	429	1983 11 7 4 42 12.54	16 30.93	120 36.95	5.00	-0.07	1.41
96	436	1983 11 7 11 2				-0.45	1.01
97	438	1983 11 7 14 32 45.45	16 7.72	120 31.09	18.42	0.87	1.72
98	439	1983 11 7 15 39				0.02	1.19
99	457	1983 11 8 8 45 19.28	16 7.29	120 32.19	32.39	1.06	1.70
100	466	1983 11 8 15 42 59.56	16 21.35	120 38.55	50.77	1.24	2.18

No.	Eq. No.	Time of Commencement	Hypocentral Coordinate			Magnitude	
			Lat.	Lon.	Depth	Tsumura	Watanabe
101	479	1983 11 9 10 27				1.20	1.93
102	481	1983 11 9 20 15 15.81	16 36.45	120 40.13	10.20	2.51	1.67
103	494	1983 11 10 16 2 46.30	16 38.99	120 40.13	18.19	2.10	2.23
104	498	1983 11 10 20 52 41.39	16 27.21	120 21.61	38.49	0.86	2.01
105	505	1983 11 11 1 49 35.77	16 25.13	120 34.86	15.66	-0.26	1.16
106	509	1983 11 11 4 54 37.49	16 5.50	120 35.77	28.95	0.35	1.23
107	513	1983 11 11 10 52 30.30	16 34.26	120 41.08	24.04	0.86	2.07
108	514	1983 11 11 11 38				0.53	1.92
109	517	1983 11 11 12 42 17.23	16 22.58	120 41.30	18.20	-0.61	1.18
110	524	1983 11 11 21 36 50.50	16 25.26	120 23.15	34.96	0.82	1.89
111	525	1983 11 11 23 59 3.21	16 14.22	120 25.02	23.55	2.02	2.37
112	539	1983 11 13 3 9 28.14	16 18.22	120 28.38	24.69	0.10	1.16
113	555	1983 11 14 2 36 40.31	16 26.97	120 34.88	16.47	-0.30	1.30
114	558	1983 11 14 6 37 25.68	16 30.07	120 26.44	23.46	2.31	2.46
115	560	1983 11 14 11 53				-0.30	0.73
116	561	1983 11 14 12 42 13.77	16 32.39	120 41.08	13.69	-0.55	1.06
117	563	1983 11 14 18 36 0.20	16 28.93	120 38.98	2.48	0.09	1.29
118	579	1983 11 15 5 57 55.24	16 21.28	120 40.01	20.07	0.83	1.82
119	582	1983 11 15 7 49 36.06	16 26.10	120 38.21	6.70	2.54	2.48
120	589	1983 11 15 18 18				-1.11	0.32
121	591	1983 11 15 19 45 23.51	16 27.09	120 39.55	7.20	1.92	2.13
122	592	1983 11 15 20 41 15.11	16 27.69	120 39.59	3.42	1.50	2.05
123	594	1983 11 15 22 54 42.71	16 27.20	120 40.13	1.70	-0.35	1.45
124	596	1983 11 16 1 20 52.61	16 37.67	120 35.10	34.64	0.93	2.04
125	601	1983 11 16 2 34 56.13	16 21.35	120 22.01	37.05	1.26	1.63
126	609	1983 11 16 11 11 49.78	16 19.10	120 42.12	6.02	-0.40	0.86
127	618	1983 11 16 20 17 56.43	16 28.94	120 39.88	2.33	0.11	1.66
128	619	1983 11 16 20 17 50.89	16 28.36	120 39.63	4.09	-1.18	1.20
129	620	1983 11 16 20 19				-0.05	1.11
130	621	1983 11 16 20 37 0.18	16 26.86	120 41.08	10.13	-0.12	1.24
131	623	1983 11 16 21 18 3.71	16 28.44	120 37.29	6.90	-0.42	1.37
132	625	1983 11 16 22 30 18.73	16 10.79	120 36.64	23.32	1.48	2.13
133	634	1983 11 17 9 17				-0.05	1.22
134	635	1983 11 17 10 14				-0.57	0.56
135	637	1983 11 17 16 59				1.47	1.81
136	642	1983 11 18 4 51 11.60	16 19.74	120 51.81	25.65	2.00	2.36
137	646	1983 11 18 11 49				0.32	1.27
138	647	1983 11 18 15 51 25.96	16 25.19	120 42.18	9.97	-0.15	1.44
139	652	1983 11 18 20 41 58.41	16 21.35	120 38.55	39.45	2.49	2.38
140	662	1983 11 19 12 35 26.87	16 21.28	120 40.01	33.68	3.50	2.08
141	664	1983 11 19 13 35 11.16	16 27.97	120 38.60	3.77	0.01	1.14
142	673	1983 11 20 7 40				-0.08	1.42
143	676	1983 11 20 13 44 35.06	16 26.14	120 42.02	10.24	-0.48	1.46
144	680	1983 11 20 15 35 41.22	16 24.55	120 40.13	7.48	-0.19	1.39
145	685	1983 11 21 1 47 44.10	16 28.78	120 41.27	2.33	-1.07	0.51
146	690	1983 11 21 13 29 40.63	16 26.48	120 56.09	30.63	2.39	2.39
147	691	1983 11 21 15 13 24.26	16 27.96	120 31.20	21.95	0.10	1.58
148	694	1983 11 22 2 22				-0.05	1.56
149	704	1983 11 22 16 29 35.68	16 25.45	120 40.13	7.53	0.15	1.44
150	705	1983 11 22 16 43 24.52	16 21.84	120 46.06	13.42	0.35	1.59

No.	Eq. No.	Time of Commencement	Hypocentral Coordinate			Magnitude	
			Lat.	Lon.	Depth	Tsumura	Watanabe
151	706	1983 11 22 16 48 42.14	16 25.56	120 39.42	5.03	1.00	1.75
152	707	1983 11 22 17 48 49.60	16 15.07	120 26.90	26.62	1.98	2.14
153	709	1983 11 22 23 39 58.95	16 14.06	120 38.78	17.76	1.09	1.91
154	714	1983 11 23 17 2				0.74	1.37
155	715	1983 11 23 17 3 6.64	16 14.39	120 24.85	31.91	1.45	2.52
156	717	1983 11 23 19 22 35.09	16 17.74	120 30.72	19.38	1.95	2.33
157	718	1983 11 23 20 4 26.28	16 27.12	120 41.08	15.02	-0.28	1.29
158	719	1983 11 23 21 20 7.08	16 25.72	120 35.87	13.39	-1.13	1.13
159	723	1983 11 24 1 27 27.51	16 29.16	120 38.69	1.84	-0.35	1.55
160	728	1983 11 24 3 29 13.32	16 27.41	120 34.67	12.23	0.46	1.86
161	735	1983 11 24 22 38 45.83	16 25.95	120 38.12	5.75	-0.20	0.66
162	736	1983 11 25 1 15 7.33	16 30.09	120 37.88	1.19	-0.37	1.37
163	737	1983 11 25 2 21 30.10	16 24.97	120 25.60	29.51	0.73	1.38
164	739	1983 11 25 4 6 55.00	16 21.28	120 40.01	19.86	0.33	1.61
165	742	1983 11 25 8 58				0.47	1.32
166	743	1983 11 25 13 19 58.99	16 21.35	120 39.65	18.65	0.69	2.04
167	756	1983 11 26 6 4 54.55	16 17.84	120 26.14	25.49	2.35	2.37
168	757	1983 11 26 6 42				0.66	1.26
169	758	1983 11 26 7 7 8.66	16 26.34	120 31.12	17.63	-0.05	1.50
170	763	1983 11 26 15 50 46.97	16 28.62	120 41.48	10.36	0.27	1.76
171	771	1983 11 27 12 33 52.06	16 17.04	120 24.56	29.18	1.85	2.20
172	772	1983 11 27 13 7 4.64	16 21.35	120 49.66	22.28	0.34	1.40
173	778	1983 11 28 3 19 45.83	16 29.41	120 35.11	20.14	0.31	1.71
174	781	1983 11 28 5 0 49.84	16 25.49	120 38.41	6.80	-1.59	1.01
175	783	1983 11 28 9 22 50.34	16 20.13	120 40.05	39.77	1.46	2.02
176	785	1983 11 28 15 37 59.81	16 29.05	120 39.33	1.21	-0.95	1.27
177	788	1983 11 28 18 36				0.54	1.48
178	789	1983 11 28 18 37				1.88	2.29
179	797	1983 11 29 3 24 32.23	16 23.08	120 30.20	19.69	0.40	1.61
180	803	1983 11 29 14 45 15.58	16 26.37	120 29.15	19.16	2.31	2.32
181	805	1983 11 29 16 4 56.59	16 28.58	120 45.48	21.79		
182	808	1983 11 29 23 57 27.80	16 28.28	120 36.93	15.18	-0.42	1.25
183	812	1983 11 30 3 26 45.44	16 31.74	120 34.26	21.22	0.62	1.75
184	816	1983 11 30 5 56 23.84	16 21.35	120 30.38	19.38	1.60	2.16
185	826	1983 11 30 17 17 37.04	16 20.13	120 40.05	18.41	-0.73	0.83
186	835	1983 12 1 1 5 10.35	16 49.01	120 40.13	37.21	1.76	2.64
187	840	1983 12 1 4 45 26.42	16 31.55	120 24.21	36.56	0.87	1.74
188	841	1983 12 1 7 36 36.42	16 17.43	120 33.30	17.60	0.47	1.48
189	845	1983 12 1 13 40 53.07	16 13.71	120 38.89	9.03	0.88	1.52
190	847	1983 12 1 14 18 30.60	16 16.07	120 39.03	11.93	0.81	1.79
191	855	1983 12 1 21 49 6.76	16 28.63	120 29.34	23.40	1.82	2.18
192	868	1983 12 2 12 39 53.05	16 11.63	120 23.65	22.73	2.22	2.45
193	870	1983 12 2 18 38				0.72	0.92
194	874	1983 12 2 22 13 16.38	16 19.72	120 39.44	4.45	-0.53	1.00
195	876	1983 12 2 23 36 20.90	16 20.13	120 40.05	22.76	0.14	1.43
196	879	1983 12 3 1 20 3.09	16 32.48	120 50.76	29.51	1.55	1.91
197	890	1983 12 3 7 27 42.67	16 6.17	120 33.60	35.76	2.51	2.41
198	903	1983 12 4 0 12 58.49	16 27.43	120 31.84	20.34	1.96	2.15
199	915	1983 12 4 12 43 11.70	16 20.13	120 40.05	22.28	0.87	2.07
200	932	1983 12 6 7 50 13.13	16 29.59	120 38.31	7.87	0.37	2.02

No.	Eq. No.	Time of Commencement	Hypocentral Coordinate			Magnitude	
			Lat.	Lon.	Depth	Tsumura	Watanabe
201	933	1983 12 6 7 50 7.99	16 28.36	120 38.36	9.05	1.24	2.08
202	934	1983 12 6 7 51 37.41	16 28.26	120 38.39	10.12	0.49	1.74
203	935	1983 12 6 7 53 19.50	16 28.51	120 36.99	11.27	0.13	1.22
204	943	1983 12 6 20 13				0.29	1.13
205	952	1983 12 7 13 40 33.75	16 21.28	120 38.64	9.46	0.76	1.73
206	953	1983 12 7 14 41 37.77	16 4.04	120 33.46	9.81	2.63	2.46
207	956	1983 12 7 16 31 54.45	16 28.60	120 38.40	16.15	0.31	1.46
208	957	1983 12 7 16 32 7.68	16 28.40	120 35.60	17.93	0.13	1.32
209	958	1983 12 7 16 32 43.39	16 30.58	120 37.51	9.84	1.47	1.92
210	960	1983 12 7 16 34 56.85	16 30.79	120 36.64	11.97	-0.52	1.51
211	967	1983 12 7 20 38 17.63	16 27.09	120 37.70	5.55	-0.26	0.95
212	970	1983 12 7 22 16 24.84	16 28.24	120 36.91	18.41	-0.24	1.27
213	973	1983 12 8 0 28				-0.16	0.87

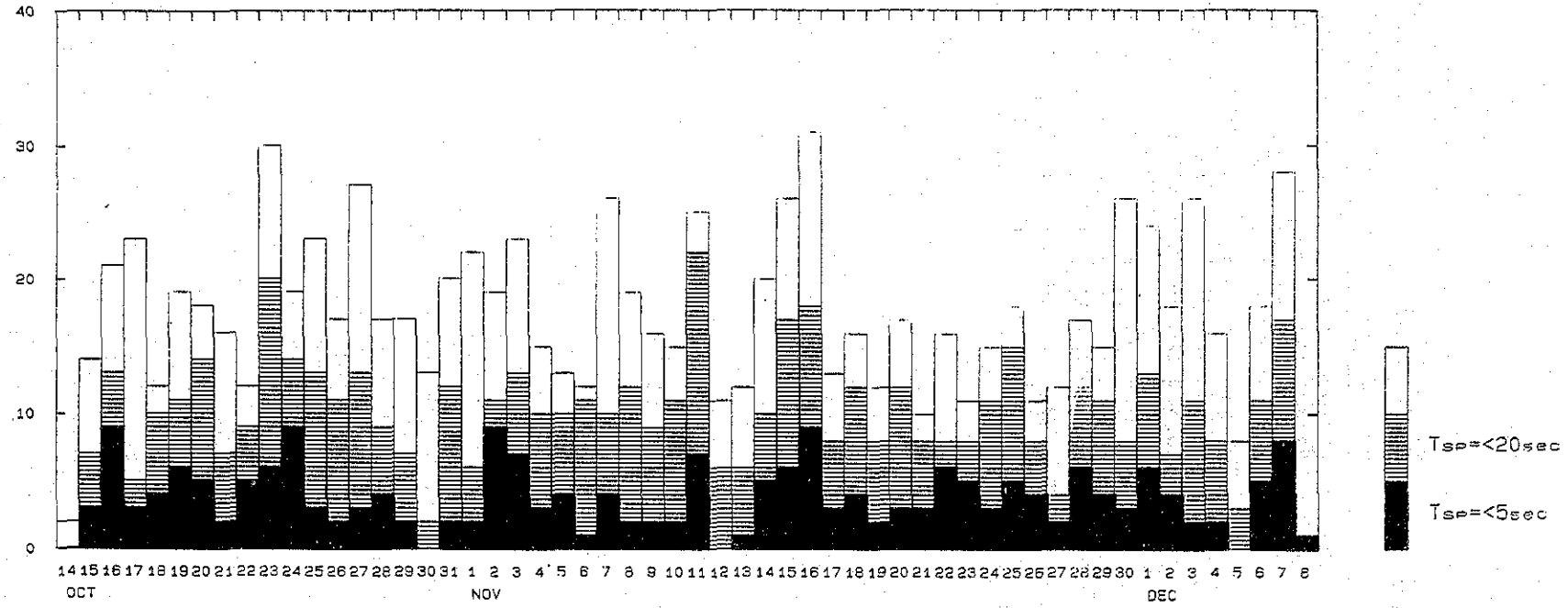

Fig. Ⅲ-3-12 Daily Frequency Diagram

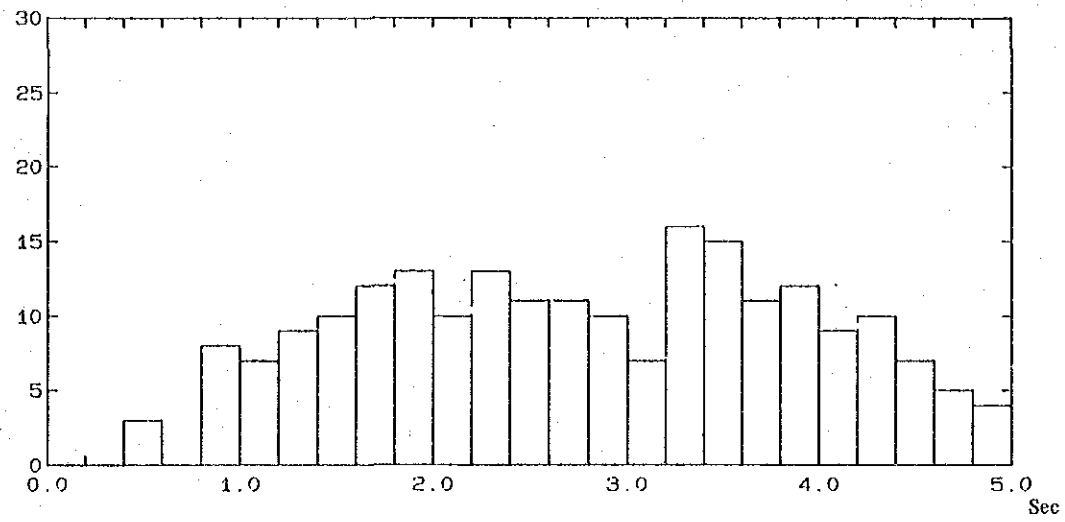

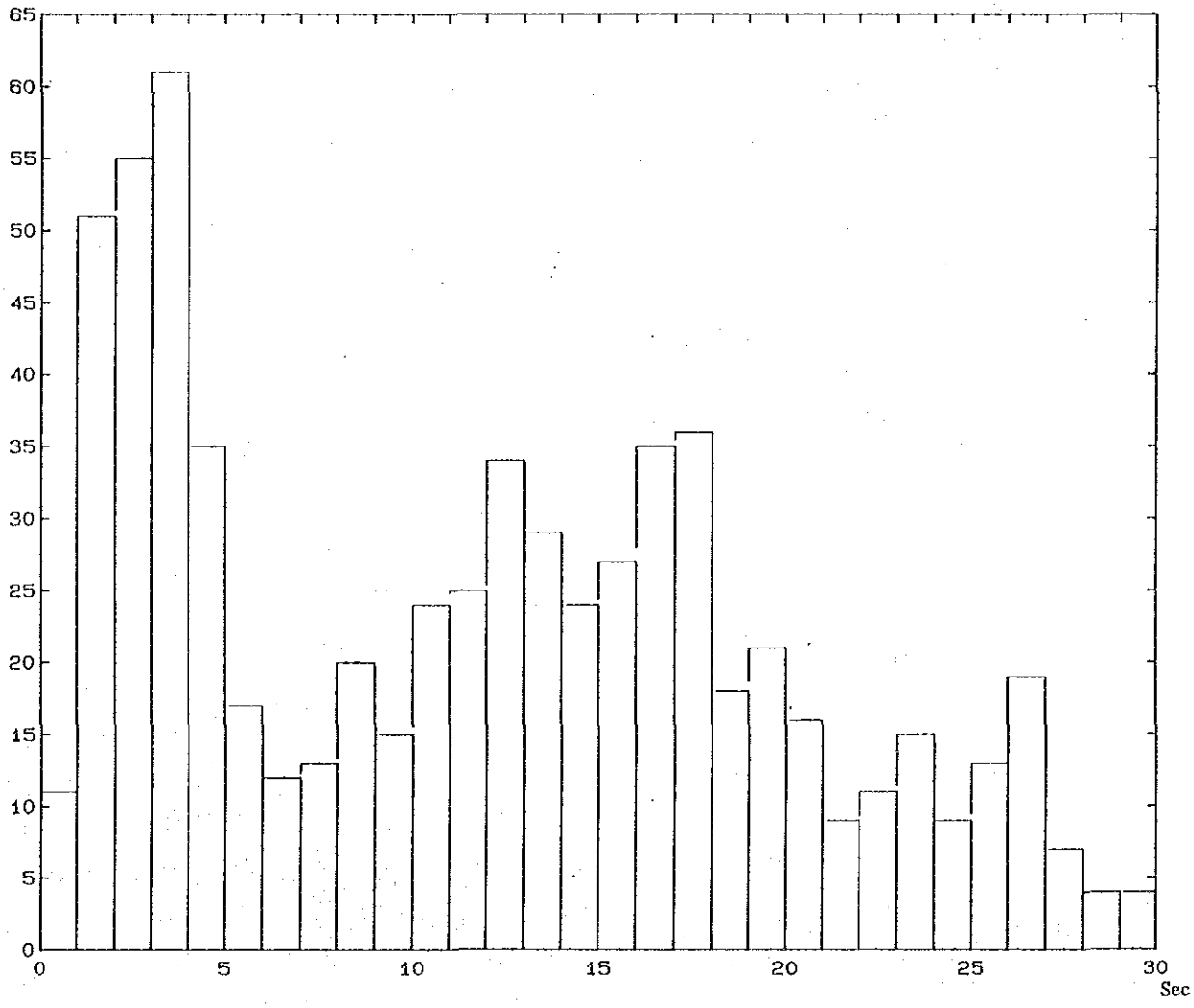

Fig. Ⅲ-3-13 S-P Time Distribution

The histogram for S-P times of 30 seconds or less show four peaks of frequency of occurrences at 1–4, 12–13, 16–18 and 26–27 seconds. The distribution is divided by one (1) second interval.

The other histogram for S-P times of 5 seconds or less is divided into 0.2 second interval and shows no significant peaks for frequency of occurrences.

3.5.3 Histograms by Magnitudes

Histograms of magnitudes derived from both Tsumura and Watanabe's equation were made at magnitude interval of 0.2 and are shown in Fig. III–3–14.

From Tsumura's method (M_T), the histogram shows normal distribution of values ranging from –0.8 to 3.6 with earthquakes of magnitudes between +0.8 and +1.0 registering the highest frequency of occurrences. On the other hand, that of Watanabe's (M_W) shows that the values distributed between 0.2 and 2.8 with two peaks at magnitudes 1.2 to 1.6 and at 2.0 to 2.2.

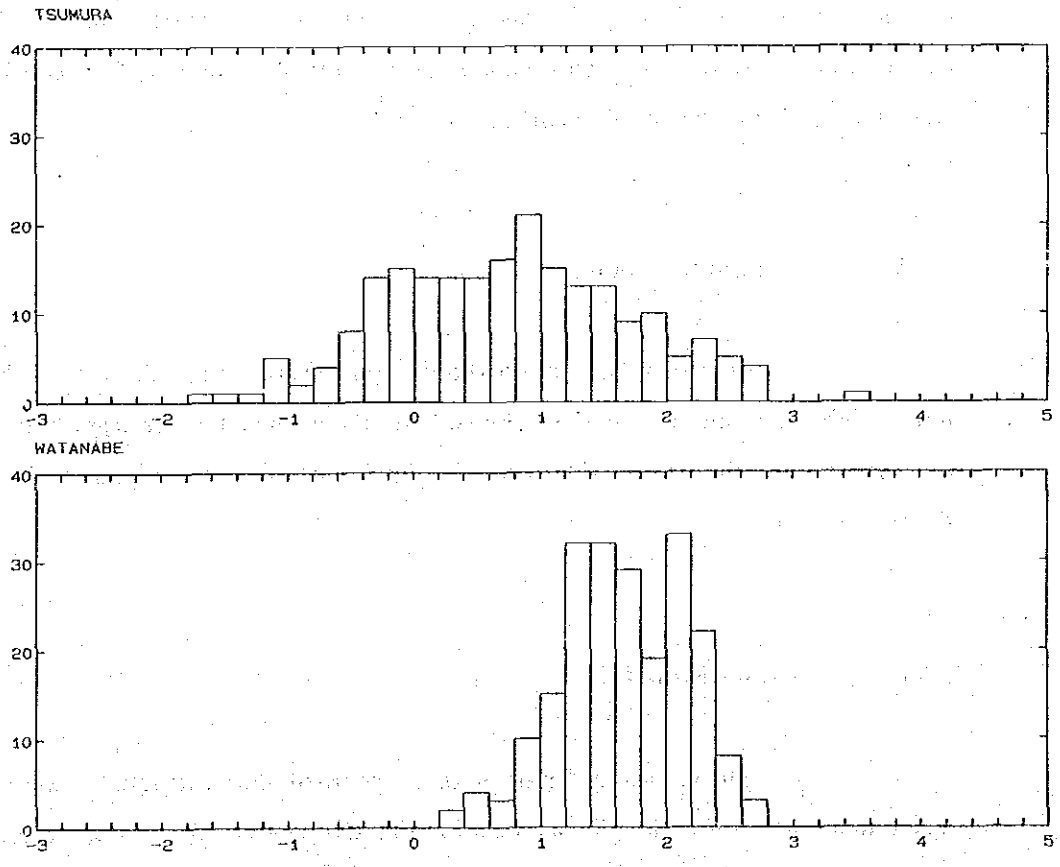

Fig. III–3–14 Magnitude Distribution

3.5.4 Spatial Distribution of Microearthqaukes

There is very little information about the P-ware velocity of the rocks in the vicinity of the survey area, so it is very difficult to assume suitable velocity constants for P and S waves. Various models of velocity structures were determined from the general P-wave velocity of diorite rocks, which are widely distributed in the area; using the values referred from the literatures. Calculations for foci of earthquakes were applied for the various models with the results analyzed and compared. Conclusively, the three-layer model was arrived at as shown below:

	P-wave Velocity (km/sec)	Thickness (km)
First layer	4.5	0.5
Second layer	6.0	9.5
Third layer	8.0	—

The average ratio of P- to S-wave velocity (Vp/Vs) in the area was derived at 1.71 using the Wadachi diagram, in which the P-wave arrival and S-P times of each earthquake were plotted with Poisson's ratio at 0.24. The foci of the earthquakes were determined by equation (7) in section 3.4.2.

3.5.5 Epicentral Distribution

Epicenters of microearthquake ($M \leq 3$) are mainly clustered within and north of the network. Except for these two areas, the epicenters are sparsely distributed. Incidentally, there were no microearthquakes that occurred east and southeast of the survey area.

3.5.6 Vertical Distribution

The vertical distribution of all recorded microearthquakes were projected in a north-south direction as shown in Fig. III–3–16. Likewise, three north-

south projections (facing east) were made between the following boundaries as shown in the same figure:

(a) 20 km-W to 5 km-W
(b) 5 km-W to 5 km-E
(c) 5 km-E to 20 km-E

In addition, four east-west projections (facing north) were made and are shown in Fig. III–3–16. One shows a east-west projection of all microearthquakes while the other three show the east-west projections from the following boundaries:

(a) 18 km-N to 5 km-N
(b) 5 km-N to 5 km-S
(c) 5 km-S to 18 km-S

On the north-south projections for all microearthquakes, the hypocenters are mostly grouped in the vicinity and north of 10 km-N ranging in depth from 0–20 kilometers. This area is north-northwest of Antamok mines. The eastern side shows there are few hypocenters. The distribution shows the central part to be the most active with hypocenters ranging from 0–12 km-N and around 10 km-N. In the western side, they are distributed at depths of more than 10 kilometers in the same area. Apparently, the hypocentral distribution shows a structure dipping to the west from the central part.

The east-west projections for all hypocenters shows the distribution dipping to the west from the central part with the width of about 10 kilometers, and concentrated at depths of less than 10 kilometers. The locations of the foci can be easily seen in detail from the north-south projections. It can be further concluded that the microearthquakes are more prevalent north of the network.

The general locations of microearthquakes in the area can be divided into three active and blank zones as follows:

Active Zone I: The zone in the vicinity of the network in which the hypocenters are discretely distributed.

Active Zone II: The zone located 5–15 km-north of the network where the hypocenters are concentrated at depths of about 10 kilometers.

Active Zone III: The zone located about 10 km-north of the network with foci distributed in a fan-shaped area dipping to the west.

Blank Zone A: The vertical cylinder-like zone surrounding the network.

Blank Zone B: The zone that covers the whole eastern part of the survey area.

Blank Zone C: The zone that corresponds to the southwestern part of the survey area.

Microearthquakes that occurred in Zone I surrounded a vertical cylinder-like structure which may correspond to a plug believed to be the heat source of the geothermal area.

Active Zones II and III, distributed north of the network may be a part of the eastern rim of a basin structure located northwest and outside the survey area. The weak zone in the vicinity of this rim might have caused the microearthquakes at these zones.

Blank Zone B corresponds to the Agno batholith which is distributed in the north-south direction at the eastern side of the survey area. This may have continued at depths since no microearthquakes were observed downward.

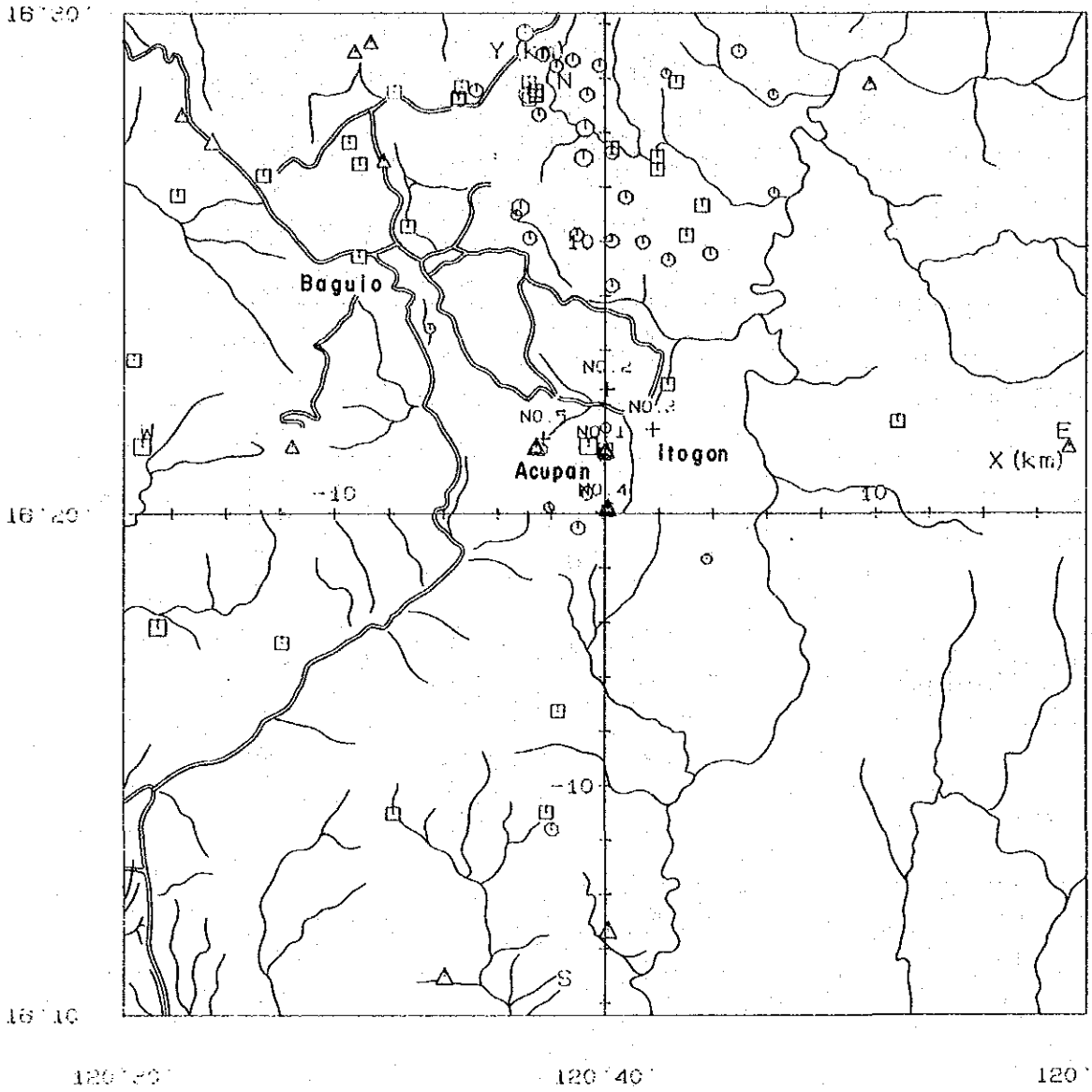

No.1
+ Seismograph

Depth (Z) \ Magnitude (M)	0≦M<1	1≦M<2	2≦M<3
0<Z≦10	⊙	⊙	⊙
10<Z≦20	□	□	□
20<Z	△	△	△

Fig. Ⅲ-3-15 Epicentral Distribution

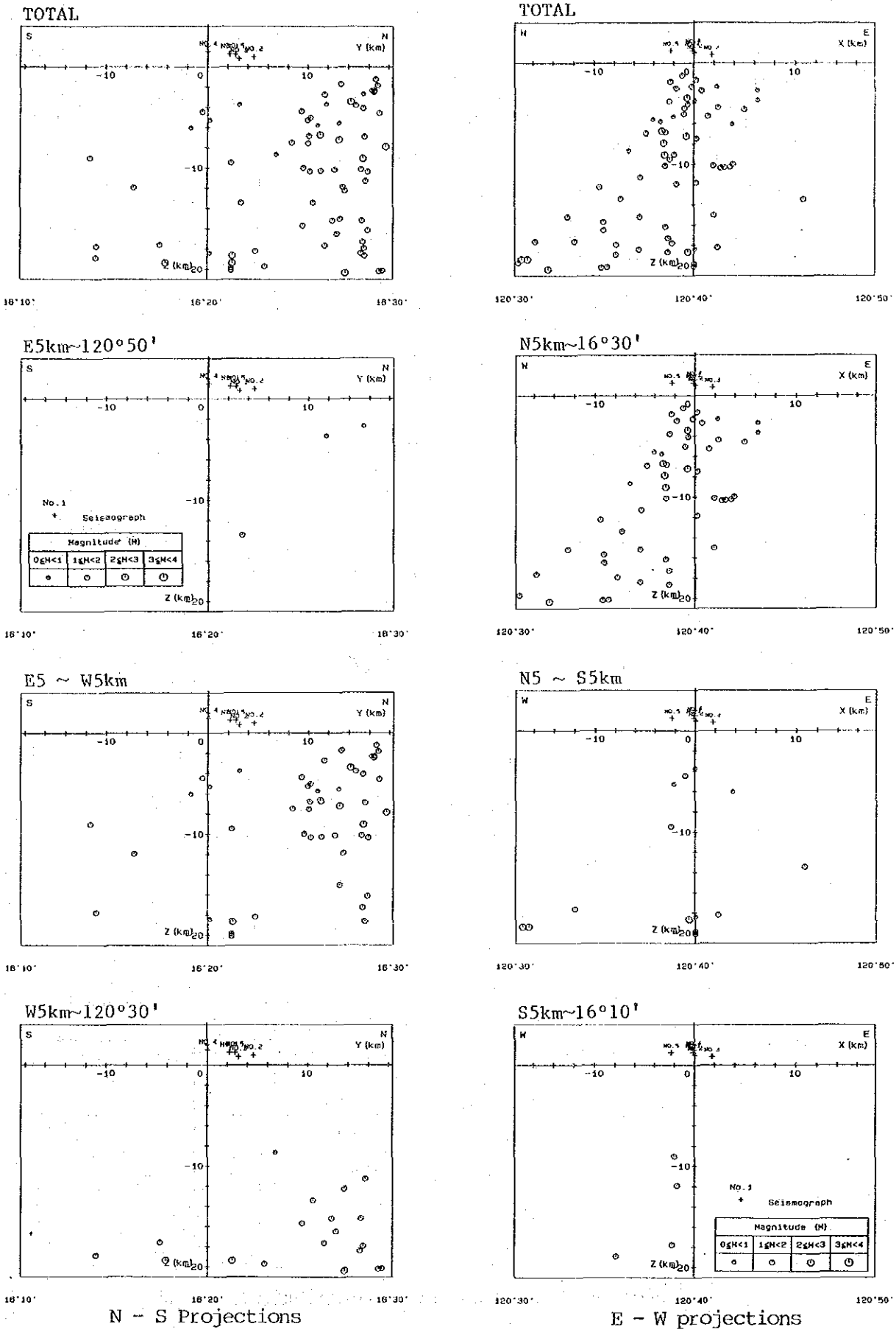

N - S Projections

E - W projections

Fig. Ⅲ-3-16 Hypocentral Distribution (E-W, N-S, Projections)